

Characterization of the Thioredoxin System of *Methanosarcina mazei*

Usha Loganathan

Thesis submitted to the faculty of Virginia Polytechnic Institute and State University in partial fulfillment of the requirements for the degree of

Master of Science

In

Biological Sciences

Committee:

Dr. Biswarup Mukhopadhyay, Chair

Dr. David L. Popham, Co-Chair

Dr. Birgit Scharf

December 1, 2014
Blacksburg, Virginia

Key words: Methane, fuel, greenhouse gas, Methanogen, Archaea, *Methanosarcina mazei*, thioredoxin, NADPH thioredoxin reductase, ferredoxin thioredoxin reductase, oxidative stress, redox regulation.

Copyright 2014, Usha Loganathan

Characterization of the thioredoxin system of *Methanosarcina mazei*

Usha Loganathan

ABSTRACT

Thioredoxin (Trx) and thioredoxin reductase (TrxR) along with an electron donor form a thioredoxin system. Such systems are widely distributed among the organisms belonging to the three domains of life. It is one of the major disulfide reducing systems, which provides electrons to several enzymes, such as ribonucleotide reductase, methionine sulfoxide reductase and glutathione peroxidase to name a few. It also plays an important role in combating oxidative stress and redox regulation of metabolism. Trx is a small redox protein, about 12 kDa in size, with an active site motif of Cys-X-X-Cys. The reduction of the disulfide in Trx is catalyzed by TrxR. Two types of thioredoxin reductases are known, namely NADPH thioredoxin reductase (NTR) with NADPH as the electron donor and ferredoxin thioredoxin reductase (FTR) which depends on reduced ferredoxin as electron donor. Although NTR is widely distributed in the three domains of life, it is absent in some archaea, whereas FTRs are mostly found in plants, photosynthetic eukaryotes, cyanobacteria, and some archaea.

The thioredoxin system has been well studied in plants, mammals, and a few bacteria, but not much is known about the archaeal thioredoxin system. Our laboratory has been studying the thioredoxin systems of methanogenic archaea, and a major focus has been on *Methanocaldococcus jannaschii*, a deeply rooted archaeon that has two Trxs and one TrxR. My thesis research concerns the thioredoxin system of the late evolving members of the group which are exposed to oxygen more frequently than the deeply rooted members of the group, and have several Trxs and TrxRs. *Methanosarcina mazei* is one such organism, whose thioredoxin system is composed of one NTR, two FTRs, and five Trx homologs.

Characterization of the components of a thioredoxin system sets the basis to further explore its function. I have expressed in *Escherichia coli* and purified the five Trxs and three TrxRs of *M. mazei*. I have shown the disulfide reductase activities in MM_Trx1 and MM_Trx5 by their ability to reduce insulin with DTT as the electron donor, and that in MM_Trx3 through the reduction of DTNB by this protein with NADPH as the electron donor, and in the presence of NTR as the enzyme. MM_Trx3 was found to be the only *M. mazei* thioredoxin to accept electrons through the NTR, and to form a complete Trx - NTR system. The Trx - FTR systems are well studied in plants, and such a system is yet to be defined in archaea. I have proposed a mechanism of action for one of the FTRs. FTR2 harbors a rubredoxin domain, and this unit is the only rubredoxin in this organism. Superoxide reductase, an enzyme that reduces superoxide radical to hydrogen peroxide without forming oxygen, utilizes rubredoxin as the direct electron source and this enzyme is found in certain anaerobes, including *Methanoscincina* species. Thus, it is possible that FTR2 provides electrons via a Trx to the superoxide reductase of *M. mazei*. This activity will define FTR2 as a tool in combating oxidative stress in *M. mazei*.

In my thesis research I have laid a foundation to understand a complex thioredoxin system of *M. mazei*, to find the role of each Trx and TrxR, and to explore their involvement in oxidative stress and redox regulation.

DEDICATION

In memory of my loving husband. To my daughters Uma and Abhi.

ACKNOWLEDGEMENTS

My deepest gratitude and thanks to Dr. Biswarup Mukhopadhyay who has been my advisor, not only through my graduate schooling but also my personal life. The word ‘thanks’ does not do justice for all that he has done for me and my children. He reached out to me when I needed help the most in my life, which I can never forget. He has spent a lot of his valuable time to patiently teach me. He continues to guide me and my children, and I greatly value his opinion and friendship. No amount of words can repay the kindness and help I have received from him. Thank you for believing that I can do it.

I thank my committee members Drs. Birgit Scharf and David Popham for serving in my committee, for encouraging and guiding me through my graduate school, and for their valuable time, advice and patience.

I thank Dr. Ruth A. Schmitz - Streit at University of Kiel, Germany, for providing the preliminary data on growth of *Methanosarcina mazei* under oxygen sensitive conditions, and for providing the clones for the NADPH thioredoxin reductase, ferredoxin thioredoxin reductases and one of the thioredoxins.

I thank Dr. Bob B. Buchanan of University of California, Berkeley, for the gift of purified spinach ferredoxin NADPH oxidoreductase (FNR).

I thank Dr. Jiann-Shin Chen of Virginia Tech, Blacksburg for his gift of purified clostridial ferredoxin and hydrogenase.

I thank Virginia Bioinformatics Institute, the Department of Biochemistry, the Department of Biological Sciences, and Virginia Tech for giving me the opportunity to pursue my Masters.

I thank my lab members Dr. Endang Purwantini, Dr. Dwi Susanti and Jason Rodriguez who have become my very close friends, and are always there to help, support, guide and give me suggestions. My

special thanks to Dwi who has been mentoring me since the day I joined Biswarup's lab. I have learned a lot from her over the years. She has helped me get through the rough times of my life. Thank you for cheering me on. Thank you all for being a wonderful friend.

I thank my two wonderful daughters, Uma and Abhi, who have stood by me, encouraging and cheering me as I walked through this path. I could not have done it without their support.

I thank the community of Virginia Tech and the New River Valley for their kindness and support through the past few years.

I have been blessed with the friendship, kindness and support from everyone on earth. I am eternally grateful for all that I have received. I thank you all from the bottom of my heart.

TABLE OF CONTENTS

ABSTRACT.....	ii
DEDICATION.....	iv
ACKNOWLEDGEMENTS.....	v
TABLE OF CONTENTS.....	vii
LIST OF FIGURES.....	x
LIST OF TABLES.....	xiv
Chapter 1: LITERATURE REVIEW	1
OXIDATIVE STRESS IN METHANOGENIC ARCHAEA.....	1
METHANOGENS	1
OXIDATIVE STRESS	3
THIOREDOXIN SYSTEM.....	9
RESEARCH INTRODUCTION	13
RESEARCH OBJECTIVES	14
Chapter 2: MATERIALS AND METHODS	17
Construction of vectors for the expression of <i>M. mazei</i> NTR, FTRs, and Trxs in <i>E. coli</i>	17
Expression of <i>M. mazei</i> Trxs, NTR, and FTRs in <i>E. coli</i>	17
Purification of the recombinant proteins	18
Western blot	20

State of oxidation of <i>M. mazei</i> Trxs	20
Oxidation and reduction of <i>M. mazei</i> Trxs.....	21
Analysis of oxidized and re-reduced Trx preparations	21
Insulin Reduction Assay for Trxs	22
Growth of <i>Methanosa</i> <i>r</i> cina <i>mazei</i>	22
RT-PCR of <i>ntr</i> (<i>mm_2353</i>) and <i>trx</i> (<i>mm_2354</i>) mRNA	22
Amino acid sequence alignment.....	22
Reconstitution of MM_NTR with Flavin Adenine Dinucleotide (FAD).....	23
UV visible spectroscopy with NTR and FTR.....	23
DTNB Reduction Assay for NTR.....	23
FTR assays:	25
Insulin reduction assay with dithionite as the electron donor	25
Insulin reduction assay with clostridial ferredoxin and hydrogenase for electron delivery	25
DTNB assay for FTR2 with spinach FNR and NADPH for electron delivery.....	25
Chapter 3: RESULTS.....	27
Structural and functional characteristics of the thioredoxins and thioredoxin reductases of <i>M. mazei</i>	28
Primary structure characteristics of the thioredoxins of <i>M. mazei</i>	28
Primary structure characteristics of NADPH thioredoxin reductase (NTR) of <i>M. mazei</i>	28
Primary structure characteristics of ferredoxin thioredoxin reductases (FTR) of <i>M. mazei</i>	29
Experimentally determined characteristics of the Trxs and TrxRs of <i>M. mazei</i>	34

Oxidation and reduction of Trxs	35
Insulin disulfide reducing activities of Trxs with DTT as electron donor	35
Pairing of <i>M. mazei</i> TrxRs with its cognate Trxs	59
DTNB assay to pair <i>M. mazei</i> NTR (MM_NTR) with its cognate Trx	59
Pairing of <i>M. mazei</i> FTR1 and 2 with its cognate Trx.....	59
Dithionite as electron donor for insulin reduction	59
Clostridial ferredoxin as the electron donor for insulin reduction	59
NADPH as the electron donor for the rubredoxin domain in FTR2 for the reduction of DTNB	60
Chapter 4: DISCUSSION.....	64
Thioredoxin and thioredoxin reductase homologs in <i>Methanosarcina mazei</i>	64
Characteristics of <i>M. mazei</i> thioredoxins	65
Thioredoxin – thioredoxin reductase systems of <i>Methanosarcina mazei</i>	67
CONCLUSION.....	71
REFERENCES	73

LIST OF FIGURES

Chapter 1	1
Figure 1. The thioredoxin system.....	11
Figure 2. Schematic representation of an NADPH – thioredoxin system involved in oxidative stress defense.....	11
Figure 3. Distribution of Trx, FTR, and NTR in methanogenic archaea	15
Figure 4. Growth pattern of <i>Methanosarcina mazei</i> under anaerobic and oxygen exposed conditions	16
Chapter 2	17
Figure 5. Insulin reduction by Trx with DTT as the electron donor	24
Figure 6. DTNB reduction assay for NTR	24
Figure 7. Insulin reduction assay for FTR	26
Figure 8. Insulin reduction for FTR with hydrogen as the electron donor.....	26
Figure 9. DTNB reduction assay for FTR2.....	27
Chapter 3	28
Figure 10. Multiple sequence alignment of the thioredoxins (Trxs) of <i>Methanosarcina mazei</i> , <i>Escherichia coli</i> , and <i>Methanocaldococcus jannaschii</i>	30
Figure 11. Multiple sequence alignment of NADPH thioredoxin reductase (NTR) from <i>Methanosarcina mazei</i> , <i>Escherichia coli</i> , and <i>Methanocaldococcus jannaschii</i>	31

Figure 12. Multiple sequence alignment of ferredoxin thioredoxin reductase-1 (FTR1) of <i>Methanosa</i> <i>r</i> cina <i>mazei</i> , and respective homologs in <i>Methanosa</i> <i>r</i> cina <i>acetivorans</i> , and <i>Methanosa</i> <i>r</i> cina <i>barkeri</i>	32
Figure 13. Multiple sequence alignment of ferredoxin thioredoxin reductase-2 (FTR2) of <i>Methanosa</i> <i>r</i> cina <i>mazei</i> , <i>Methanosa</i> <i>r</i> cina <i>acetivorans</i> , and <i>Methanosa</i> <i>r</i> cina <i>barkeri</i>	33
Figure 14. Schematic representation of the operon type arrangement of <i>mm_2353 (ntr)</i> and <i>mm_2354 (mm_trx5)</i> of <i>Methanosa</i> <i>r</i> cina <i>mazei</i>	37
Figure 15. RT-PCR analysis of <i>mm_2353 (ntr)</i> and <i>mm_2354 (mm_trx5)</i> mRNA targeting the respective junction	37
Figure 16. Expression of <i>M. mazei</i> NTR (MM_2353) in <i>E. coli</i>	38
Figure 17. Expression of <i>M. mazei</i> FTR1 (MM_0057) in <i>E. coli</i> and examining its solubility	39
Figure 18. Expression of <i>M. mazei</i> FTR2 (MM_3270) and its solubility in <i>E. coli</i>	40
Figure 19. Expression of <i>M. mazei</i> MM_Trx1 (MM_0436) and its solubility in <i>E. coli</i>	41
Figure 20. Expression of <i>M. mazei</i> MM_Trx2 (MM_0737) and its solubility in <i>E. coli</i>	42
Figure 21. Expression of <i>M. mazei</i> MM_Trx3 (MM_2079) and its solubility in <i>E. coli</i>	43
Figure 22. Expression of <i>M. mazei</i> MM_Trx4 (MM_2249) and its solubility in <i>E. coli</i>	44
Figure 23. Expression of <i>M. mazei</i> MM_Trx5 (MM_2354) in <i>E. coli</i> strains BL21(DE3) and C41(DE3)...	45
Figure 24. Purification of recombinant <i>M. mazei</i> NTR (MM_2353) via Ni ²⁺ - affinity chromatography.	46
Figure 25. Purification of recombinant <i>M. mazei</i> FTR1 (MM_0057)via Ni ²⁺ - affinity chromatography.	47
Figure 26. Purification of recombinant <i>M. mazei</i> FTR2 (MM_3270) via Ni ²⁺ - affinity chromatography	48

Figure 27. Purification of recombinant <i>M. mazei</i> MM_Trx1 (MM_0436) via Ni ²⁺ - affinity chromatography	49
Figure 28. Purification of recombinant <i>M. mazei</i> MM_Trx2 (MM_0737) via Ni ²⁺ - affinity chromatography	50
Figure 29. Purification of recombinant <i>M. mazei</i> MM_Trx3 (MM_2079) via Ni ²⁺ - affinity chromatography	51
Figure 30. Purification of recombinant <i>M. mazei</i> MM_Trx4 (MM_2249) via Ni ²⁺ - affinity chromatography	52
Figure 31. Purification of recombinant <i>M. mazei</i> MM_Trx5 (MM_2354) via Ni ²⁺ - affinity chromatography	53
Figure 32. UV visible spectra of <i>M. mazei</i> NTR (MM_2353) as purified and after reconstitution with FAD	54
Figure 33. UV visible spectroscopy of <i>M. mazei</i> FTR1 (MM_0057) and FTR2 (MM_3270)	55
Figure 34. Oxidation and reduction of <i>M. mazei</i> MM_Trx3 (MM_2079)	56
Figure 35. Insulin reduction activity of <i>Methanosarcina mazei</i> Trxs and <i>Escherichia coli</i> Trx (EcTrx) with DTT as the electron donor	57
Figure 36. Insulin reduction activity for the Trxs of <i>Methanosarcina mazei</i> and <i>Escherichia coli</i> Trx (EcTrx)	58
Figure 37. DTNB reduction activity of <i>Methanosarcina mazei</i> Trxs and <i>Escherichia coli</i> Trx (EcTrx) with <i>M. mazei</i> NTR as the electron transfer enzyme.....	61
Figure 38. DTNB reduction activities of Trxs from <i>Methanosarcina mazei</i> (MM_Trx1 - 5) and <i>Escherichia coli</i> Trx (EcTrx) with <i>M. mazei</i> NTR as the electron transfer enzyme	62

Figure 39. DTNB reduction activities of <i>Escherichia coli</i> Trx (EcTrx) and <i>Methanosarcina mazei</i> Trxs with <i>E. coli</i> NTR as the electron transfer enzyme	63
Chapter 4	64

Figure 40. Proposed utilities for FTR2 – Trx/Grx systems in <i>Methanosarcina mazei</i>	69
---	----

LIST OF TABLES

Table 1. List of primers for amplifying Trx and TrxR coding sequences.....	19
Table 2. Characteristics of the thioredoxin system of <i>Methanosarcina mazei</i>	72

Chapter 1: LITERATURE REVIEW

OXIDATIVE STRESS IN METHANOGENIC ARCHAEA

METHANOGENS

Methanogens are strict anaerobes that belong to the domain of Archaea and produce methane as the end product of their energy metabolism [2]. These organisms are found in a variety of habitats, such as the termite hind-gut, rumen of ruminating animals, the large intestine of humans, wet wood of trees, rice paddy fields, marshes, pond sediments, deep sea hydrothermal vents, and sewage sludge digesters [3, 4]. Their growth temperatures range from < 0°C to 110°C [2]. The psychrophilic methanogen, *Methanogenium frigidum*, which was isolated from the Ace Lake in Antarctica, has been shown to grow at a temperature range of 17°C to < 0°C [5]. Hyper-thermophilic methanogens isolated from the deep sea vents, such as *Methanopyrus kandleri*, can grow at temperatures as high as 110°C [2].

Methanogens play a major role in the global carbon cycle [3]. Carbon dioxide from the atmosphere is fixed by plants to form complex polymers which are utilized by other organisms. Under anaerobic conditions in many niches of nature, these complex organic polymers like cellulose are hydrolyzed by hydrolytic bacteria, into simple monomers such as glucose [6]. These are further broken down by fermentative bacteria to form fatty acids, alcohols, acetate and H₂ and CO₂ [7]. The fatty acids and alcohols are fermented by a group of anaerobic bacteria to form acetate and H₂ and CO₂ [6]. H₂ and CO₂ are used by the methanogens to form CH₄ and CO₂, which are released into the atmosphere as gases [6]. Acetate, the end product of many fermentative bacteria, makes the environment very acidic, a condition that is non-conducive for many organisms to grow [6]. *Methanosarcina* and *Methanotherix* species are the only methanogens that can use acetate as their methanogenic substrate [3, 6]. Methane produced in these

processes serve as a carbon and energy source for methanotrophic bacteria, which oxidize methane with oxygen and releases the carbon back to the atmosphere in the form of CO₂ gas, and thus completing the carbon cycle [6].

About a billion ton of methane is produced globally by the methanogenic archaea in the anoxic niches of nature [8]. Methane harnessed from sewage treatment plants, and landfill is used as an alternative energy source [6, 9]. Methanogenic biodegradation can be used to produce methane as fuel from renewable resource [9]. On the other hand, methane is a potent green-house gas, and from some environments methane is released to the atmosphere, contributing toward climate change and global warming [8]. Thus, methanogens play an important role in the environment and in energy production.

Methanosarcina.

Most methanogens use H₂ and CO₂, and some of them, such as *M. jannaschii*, are restricted to only these substrates for the production of methane [2]. In contrast *Methanosarcina* species, which live in moist soil, swamps, paddy fields, fresh water ponds and marine sediments, as well as in the rumen of ruminating animals and other common anaerobic environment, can use several substrates such as methanol, acetate, methylsulfides and methyl amines, often in addition to H₂ and CO₂, for methanogenesis [2, 7].

Most of the methane produced biologically on earth comes from acetate [7, 10]. *Methanosarcina* and *Methanosaeta* species are the only methanogens that can produce methane from acetate [7], making these organisms ecologically very important [11, 12]. Methane produced by the *Methanosarcina* species during the late Permian period is blamed for the extinction of more than 90% of all species on earth [11]. During that time, around 252 million years ago, the *Methanosarcina* species acquired the highly efficient acetate kinase (Ack) – phosphotransacetylase (Pta) pathway, by horizontal gene transfer from *Clostridia*

[11, 13]. These new components allow the organisms to convert acetate to acetyl CoA which then enters the methanogenesis pathway to produce methane and CO₂ [10, 14].

The size of *Methanosarcina mazei* genome is 4.1 Mbp with 1.01 Mbp of non-coding region [15]. The genome is twice that of the deeply rooted methanogen, *Methanocaldococcus jannaschii* [15]. *M. mazei* genome has 3,371 open reading frames (ORF), of which 376 ORFs are unique to the *Methanosarcina* species. 1,043 ORFs have close bacterial homologs, which is the largest among methanogenic archaea [15]. In contrast, *M. jannaschii* has a total of 1,738 identified ORFs, of which only 239 ORFs have bacterial homologs [15, 16]. *M. mazei*'s bacterial type genes are closely related to anaerobic bacteria such as *Clostridium* species, facultative bacteria, and cyanobacteria [15]. *Methanosarcina* uses both bacterial and archaeal proteins in the metabolic pathways for energy production, and carbon and nitrogen assimilation. Many of the genes involved in the methanogenesis pathway are unique to archaea [15]. In *M. mazei*, the organism uses a bacterial type of acetate kinase and phosphotransacetylase for activation of acetate to acetyl CoA, whereas the genes for carbon monoxide dehydrogenase/acetyl CoA synthase, which cleaves acetyl-CoA, are of archaeal type [14, 15]. *M. mazei* genome also has a large number of insertion sequence (IS) elements and transposases which indicates that the organism has obtained many of the genes via lateral gene transfer [15].

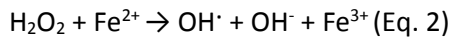
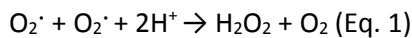
OXIDATIVE STRESS

Formation of Reactive Oxygen Species

The toxic effects of oxygen on a cell, caused by the generation of reactive oxygen species (ROS), such as the superoxide radical (O₂[·]), hydroxyl radical (OH[·]), and hydro-peroxyl radicals (HOO[·]), is called oxidative stress [17]. Molecular oxygen has two unpaired electrons in its outer most shell. When this ground state oxygen is reduced by one electron, the superoxide radical is formed [18]. Electrons escaping from the electron transport chains, mainly their components such as NADH dehydrogenase of Complex I

and the ubisemiquinones in Complex III, are involved in this process [19]. Enzymes such as NADH oxidase and xanthine oxidase, and auto-oxidation of intracellular compounds like reduced flavins, ubiquinols, and catechols are also sources of electrons for superoxide generation [17].

The dismutation of superoxide radicals by the enzyme superoxide dismutase (SOD) results in the formation of hydrogen peroxide (H_2O_2) (Eq. 1). In the presence of free ferrous iron which is released from the oxidation of Fe – S clusters, H_2O_2 forms the highly reactive hydroxyl radical (Eq. 2), and this process is called the Fenton reaction [20].



Damage due to reactive oxygen species

The ROS can cause extensive damage to the cell's DNA, lipids, and proteins which can ultimately lead to cell death.

DNA damage

Hydroxyl radical (OH^\cdot) produced in the Fenton reaction can cause damage to DNA [21, 22]. It reacts with the DNA bases, causing mutations and double strand DNA breaks. An example would be the formation of 8-hydroxyguanosine or thymine glycol, when OH^\cdot reacts with guanine and thymine respectively [23]. The lesions caused by the production of thymine glycol on a DNA strand leads to the $T \rightarrow C$ mutation, while 8-hydroxyguanosine formation causes $CG \rightarrow TA$ transversion [17]. 8-hydroxyguanosine formed in the promoter region can affect the binding of transcription factors, thus influencing the level of transcription [23]. DNA-protein cross linkages formed by the reaction between the aromatic amino acid residues and the altered DNA bases hinders DNA replication, which can ultimately lead to cell death [23]. Furthermore, OH^\cdot can react with the sugar moiety of the DNA and cause strand breakage [23].

Lipid peroxidation

Lipid peroxidation is very harmful to the cell. Such modifications of cell membrane lipids reduces the fluidity of the membrane, causing it to become rigid, and lose permeability, which can lead to cell death [17]. OH⁻ reacts with unsaturated fatty acids, abstracting a hydrogen from a methylene group adjacent to a double bond of the respective hydrocarbon chain and creating a carbon centered radical. Oxygen then reacts with this carbon centered radical to form the peroxy radical, which then reacts with another lipid molecule, thus causing a chain reaction and destruction of lipids [24].

Protein oxidation

When cellular proteins are exposed to ROS, the side chains of certain amino acid residues are oxidized, which alters the structure and function of the proteins, thereby affecting cellular metabolism. The changes in the amino acid side chains can cause protein – protein cross linkages and make the protein susceptible to proteolysis. Oxidation of amino acid residues can also decrease the thermo-stability of the proteins. The cysteines in many cellular proteins are often maintained in reduced form. Oxidative stress causes oxidation of the cysteine sulphydryl groups, leading to disulfide bond formation, thus changing the activities of the proteins. Oxidative modification of the amino acid residues can result in the inactivation of catalytic sites [25].

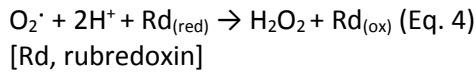
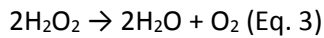
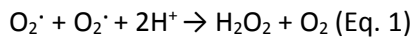
Free ferrous iron in the cell reduces molecular oxygen to form the superoxide radical and ferric iron [21]. Oxygen can also react with reduced flavin containing redox proteins, making them inactive and generating superoxide radicals or hydrogen peroxide [21]. Superoxide radicals can directly inhibit mitochondrial enzymes like NADH dehydrogenase, NADH oxidase and ATPase [21]. It reacts very rapidly with [4Fe-4S] clusters of proteins like aconitase and fumerase, [21]. Oxidation of the stable [4Fe-4S]²⁺ state of a Fe-S cluster to an unstable [4Fe-4S]³⁺, leading to the release of iron ion. The targeted protein is left

with a $[3\text{Fe}-4\text{S}]^{1+}$ cluster which makes the protein inactive. Eventually the remaining three iron atoms fall off the Fe-S cluster, destroying the protein structure completely [21].

Examples of proteins that are affected due to ROS are enolase participating in glucose catabolism, DnaK performing chaperone function, EF-G protein assisting protein synthesis, outer membrane protein Omp-A, and the β -subunit of ATPase [25]. Damage to these proteins leads to retarded cell growth or even cell death.

DEFENSE AGAINST ROS

A living cell employs various enzymes to detoxify ROS. In aerobic organisms, the enzymes superoxide dismutase (SOD) and catalase provide protection against ROS. Some anaerobic organisms, like the *Methanosarcina* species, that occasionally come across oxygen in their environment also have SOD and catalase enzymes, and these enzymes are over-expressed in these organisms during oxidative stress [26]. As mentioned above, SOD catalyzes the dismutation of O_2^\cdot (Eq. 1) to form hydrogen peroxide and molecular oxygen. Catalase detoxifies hydrogen peroxide to form water and oxygen (Eq. 3) [17]. Various peroxidases, like glutathione peroxidase or NADH peroxidase, also detoxify hydrogen peroxide [17]. In addition to these enzymes, the cell also uses low molecular weight antioxidants such as glutathione and melatonin to detoxify ROS [24]. Some of the strict anaerobes use the enzyme superoxide reductase (SOR), which generates hydrogen peroxide from superoxide without forming any oxygen in the cell (Eq. 4) [27].



Antioxidant enzymes

Superoxide dismutase

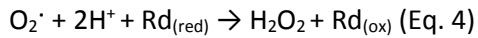
Superoxide dismutase (SOD) is found in all aerobic organisms and some anaerobic organisms. SOD undergoes successive oxidation and reduction of the transition metal ions at the active site to dismutate the superoxide radicals, forming hydrogen peroxide and oxygen. SODs are classified based on the type of metal ions of the active site. It can have single metal ion such as Fe^{2+} , Mn^{2+} , Ni^{2+} , or two metal ions $\text{Cu}^{1+}/\text{Zn}^{2+}$ [28]. In eukaryotes the SOD can be located in the cytosol or the mitochondria [28]. In bacteria it can be cytosolic or periplasmic [28]. Some of the anaerobic archaea, including the *Methanosarcina* species, which are occasionally exposed to oxygen, carry SOD with Fe^{2+} or Mn^{2+} as the cofactor, and these SODs are located in the cytosol or extracellularly [28].

Catalase

Catalase is a heme containing enzyme that catalyzes the degradation of two molecules of hydrogen peroxide to form two molecules of water and one molecule of oxygen (Eq. 3). It is found in all aerobic bacteria, eukarya and in some archaea like *Methanosarcina* species, *Methanococcus burtonii*, and *Methanobrevibacter arboriphilus* [29], but absent in deeply rooted archaea such as *Methanocaldococcus jannaschii*. This suggests that the enzyme developed at a later time as oxygen was generated on early earth [30]. There are three main evolutionary clades of the catalase superfamily: Clade 1 and 3 has small subunit catalases which are comprised of about 500 amino acid residues per subunit, and each Clade 2 enzyme has a large subunit with about 750 residues [29, 30]. The Clade 2 which includes the bacterial and fungal larger subunit catalases, represents an ancestral form. Clade 1 and 3 enzymes evolved from Clade 2 catalases. Clade 1 has mainly plant and fungi catalases. Some archaea that have catalases have the small subunit Clade 3 type enzyme, but *Methanosarcina mazei* has a large subunit Clade 2 enzyme [29].

Superoxide reductase

Superoxide reductase (SOR) is a non-heme iron containing enzyme, where the iron is not held by a porphyrin ring but rather by amino acid ligands such as His and Cys [31]. The enzyme catalyzes the reduction of superoxide to form hydrogen peroxide without the formation of oxygen. It uses rubredoxin (Rd) as the electron donor (Eq. 4) [31, 32].



This enzyme is found only in anaerobic and micro-aerophilic bacteria and archaea, and was first isolated from a sulfate reducing bacterium [32]. It has been classified into three major classes. Each has a common unit called the main domain that harbors the catalytic site with a Fe(His)₄(Cys), where the iron atom is held by four histidine residues on the equatorial plane and cysteine residue occupies the axial position [32]. Class I type SOR, also known as desulfoferredoxin, has the main domain catalytic site of Fe(His)₄(Cys), and a smaller N-terminal domain with an additional iron atom held in place by four cysteine residues [32]. Class II type SOR, called neelaredoxin for the blue color of the protein, is composed of only the main domain [32]. Class III type SOR, also called neelaredoxin and blue in color, is similar to Class I enzyme, but the N-terminal domain lacks the additional iron atom [32]. A new type of SOR, classified as Class IV enzyme has been found in the *Methanoscincina* species. This enzyme, termed as methanoferedoxin, has a catalytic site with Fe(His)₄(Cys) in the main domain, and a [4Fe-4S] cluster at the C-terminus [33].

Low molecular weight antioxidants

Detoxification of the superoxide radicals and the hydrogen peroxide is catalyzed by the enzymes SOD, SOR and catalase, but no such enzyme is known for the detoxification of the hydroxyl radicals. A group of low molecular weight antioxidants (LMWA) can prevent oxidative damage by interacting directly or indirectly with various ROS, including hydroxyl radicals. When interacting directly with ROS, the LMWAs

donate electrons to the oxygen radicals, and prevents them from causing biological damage [24]. In the indirect method the LMWAs chelate transition metals and prevent their participation in the Haber-Weiss reaction which forms the hydroxyl radicals. Glutathione is a LMWA thiol containing tri-peptide made of glutamic acid-cysteine-glycine [24]. It also acts as a chelator of metal ions. Glutathione can also detoxify hydroxyl radicals and peroxyl radicals by reducing these species. Melatonin is also a form of LMWA that can neutralize hydroxyl radicals [24].

THIOREDOXIN SYSTEM

The antioxidant enzymes and low molecular weight anitoxidants are defense tools against oxidative stress. The thioredoxin system functions as a repair mechanism for activating proteins rendered inactive due to oxidative stress. A thioredoxin system is composed of a thioredoxin (Trx), thioredoxin reductase (TrxR) and an electron donor. In this system, the Trx reduces the disulfide bonds in proteins that have been oxidized due to the presence of oxygen and in the process it gets oxidized. Thioredoxin reductase regenerates reduced Trx with an electron donor such as NADPH or ferredoxin (Figure 1) [34].

Thioredoxin

Thioredoxin is a small ubiquitous protein found in all three domains of life. It is about 12kDa in molecular mass, and carries an active site motif of Cys-X-X-Cys, which is involved in the redox reaction of Trx [35]. This protein was first discovered in *E. coli* in 1964 as an electron donor for the enzyme ribonucleotide reductase that aids in DNA synthesis [35, 36]. Thioredoxin helps the living cells to cope with oxidative stress by providing reducing power to various peroxidases, such as glutathione peroxidase or NADH peroxidase (Figure 2) [37-39]. It also serves as an electron donor for the enzymes methionine sulfoxide reductase [40] and 3-phosphoadenosine 5'-phosphosulfate (PAPS) reductase [41] which are necessary for protein repair and sulfur assimilation, respectively [40, 41]. In *Methanocaldococcus*

jannaschii the Trx1 (Mj0307) has been found to be involved in the activation of deactivated methanogenesis enzymes [42].

The primary structure of a Trx was first determined in 1968, with *E. coli* protein which has a catalytic site of CGPC [35]. The three dimensional crystal structure of this Trx was solved using X-Ray crystallography in 1975 [35]. In a Trx, five strands of β -pleated sheets form the core while four α -helices surround them, to form the basic structure that is known as the thioredoxin fold [35]. The two cysteines of the catalytic site protrude between the helices and the middle of the β -sheet strands. Proteins with the catalytic site motif of CXXC that have the thioredoxin-like fold belong to the thioredoxin superfamily and they form five major groups: thioredoxin, glutaredoxin, glutathione peroxidase, glutathione-S-transferases, and protein disulfide isomerase (PDI) [43].

Primary Electron Donor

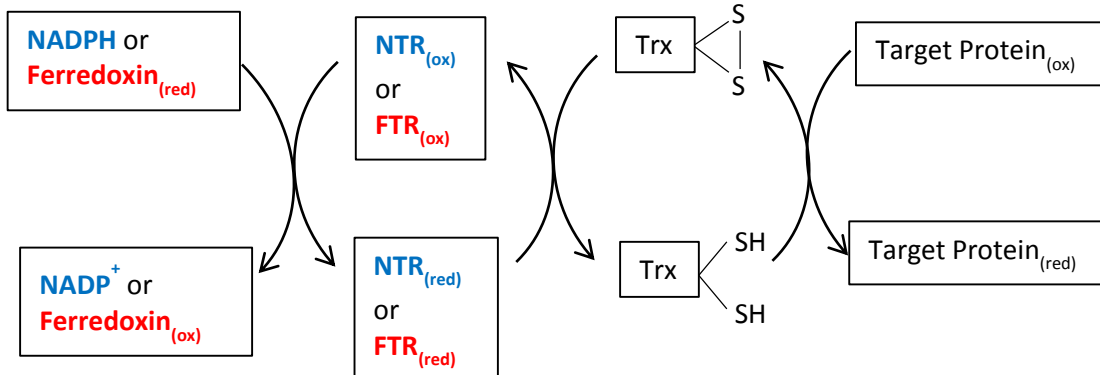


Figure 1. The thioredoxin system. Trx, Thioredoxin. NTR, NADPH-dependent Thioredoxin Reductase. FTR, Ferredoxin-dependent Thioredoxin Reductase.

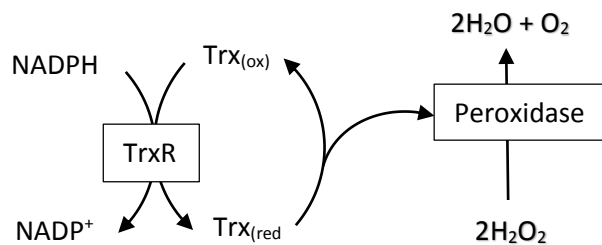


Figure 2. Schematic representation of an NADPH-dependent thioredoxin system involved in oxidative stress defense. NTR catalyzes the reduction of Trx using NADPH as the electron donor, and Trx provides electrons for the enzyme peroxidase which converts hydrogen peroxide to water and oxygen.

Various assays have been used to determine thioredoxin activity, like the methionine sulfoxide [44], ribonucleotide reductase [45], DTNB reduction [46], and insulin reduction assays [47] to name a few. The last assay provides a rapid method for spectrophotometric measurement of the disulfide reducing activity of Trx, and is the most commonly used. In this reaction disulfide bonds holding the two chains of insulin are reduced by Trx and the resulting precipitation of the two chains is observed by a change in optical density at 650nm [35, 46, 48, 49].

Thioredoxin reductase

Thioredoxin reductases (TrxR) catalyze the reduction of thioredoxins, and these enzymes are of two types, one uses NADPH as its electron donor and is known as NADPH thioredoxin reductase (NTR), and the other uses reduced ferredoxin and is known as ferredoxin thioredoxin reductase (FTR).

NADP thioredoxin reductase

The NADPH-dependent thioredoxin reductase (NTR) is a flavoprotein with an FAD prosthetic group, an NADPH binding site and an active site Cys pair [50]. The reductase transfers electrons from NADPH via FAD to reduce the active site disulfide of oxidized Trx. It was first purified from *E. coli* and its properties were described in 1964 [51].

The NTRs are classified into two types: low molecular mass and high molecular mass. The NTRs of complex eukaryotes such as humans and other mammals, drosophila, and the malaria parasite *Plasmodium falciparum*, have a larger subunit (55 kDa) [52]. The enzymes from *E. coli* and other bacteria, plants, fungi, and archaeal enzymes have a lower molecular mass subunit (35 kDa). Both types of NTRs are dimers with one FAD and one redox active Cys pair in each subunit. The high molecular mass type has an additional redox active site in each subunit, which in the case of the human enzyme contains a selenocysteine residue [53]. The NADPH binding site which is present in both high and low molecular mass thioredoxin reductases, has the conserved sequence motif of GXGXXA/G, whereas the conserved active site motif of CXXC is only present in the low molecular mass thioredoxin reductases [52].

Ferredoxin thioredoxin reductase

Ferredoxin thioredoxin reductase (FTR) uses reduced ferredoxin as electron donor. It is found in archaea, eubacteria, cyanobacteria and eukaryotic phototrophs [54]. It was first identified as the enzyme with its cognate Trx that activates fructose 1,6-bisphosphatase, a key enzyme of the Calvin-Benson Cycle in plant chloroplasts [55]. Then it was found that the FTR-Thioredoxin System (FTS) controls several other enzymes of the Calvin-Benson Cycle, namely sedoheptulose 1,6-bisphosphatase, phosphoribulokinase, NADP-glyceraldehyde 3-phosphate dehydrogenase, and Rubisco as well [55, 56]. FTR from wheat endosperm amyloplasts are found to be involved in numerous biological functions such as starch metabolism, lipid biosynthesis, carbohydrate metabolism, and amino acid synthesis [57].

FTR is a yellowish brown colored, disk shaped molecule [58]. It has two subunits – a catalytic subunit and a variable subunit. The catalytic subunit, called the beta subunit, has highly conserved cysteines which coordinate a 4Fe-4S cluster and constitutes the active site [59]. In an FTS, electrons are transferred from reduced ferredoxin via the 4Fe-4S cluster of the FTR to the cognate thioredoxin which then reduces target proteins [60]. The FTR catalytic subunits have been classified into seven different groups, based on their phylogenetic and structural characteristics [54]. The variable subunit called the alpha subunit is found in the FTR of cyanobacteria and eukaryotic phototrophs. It is thought to protect the oxygen sensitive 4Fe-4S cluster of the catalytic subunit [54].

RESEARCH INTRODUCTION

Methanoscincina mazei has five thioredoxin homologs, namely MM_0436, MM_0737, MM_2079, MM_2249, and MM_2354, and in this study these are named as MM_Trx1-5, respectively. It has one NTR homolog MM_2353 (MM_NTR), and two FTR homologs, MM_0057 (FTR1) and MM_3270 (FTR2) (Figure 3).

Methanosarcina species have been known to tolerate oxygen [61]. The unpublished collaborative work from Dr. Ruth A. Schmitz - Streit's laboratory at University of Kiel, Germany, describes *M. mazei* to be oxygen tolerant. Figure 4 shows the growth patterns of *M. mazei* under anaerobic and oxygen exposed conditions. In a transcriptomic analysis, an increase in the abundances of the mRNAs of NTR homolog (*mm_2353*) and a Trx (*mm_0436*) was observed in the oxygen exposed *M. mazei* cells. Genomic analysis indicated that MM_Trx5 (MM_2354) is probably the substrate for the NTR (MM_2353) as their genes form an operon-like arrangement. Such an assignment for MM_Trx1 – 4 could not be made.

RESEARCH OBJECTIVES

The overall objective of my thesis research was to characterize the thioredoxin system of *Methannosarcina mazei* and it had five sub-objectives:

1. To express each Trx and TrxR protein in soluble forms, and purify these to homogeneity.
2. To examine the disulfide reducing activity for each of the Trx homologs via insulin disulfide reduction assay.
3. To examine whether the TrxR homologs assemble their respective cofactors by UV visible spectrophotometric analysis.
4. To pair the individual TrxR with its cognate Trxs experimentally.
5. To perform RT-PCR analysis for the genes *mm_2354* and *mm_2353*, which encodes MM_Trx5 and the NTR of *M. mazei* to test if they belong in an operon.

Thioredoxin system in methanogenic archaea

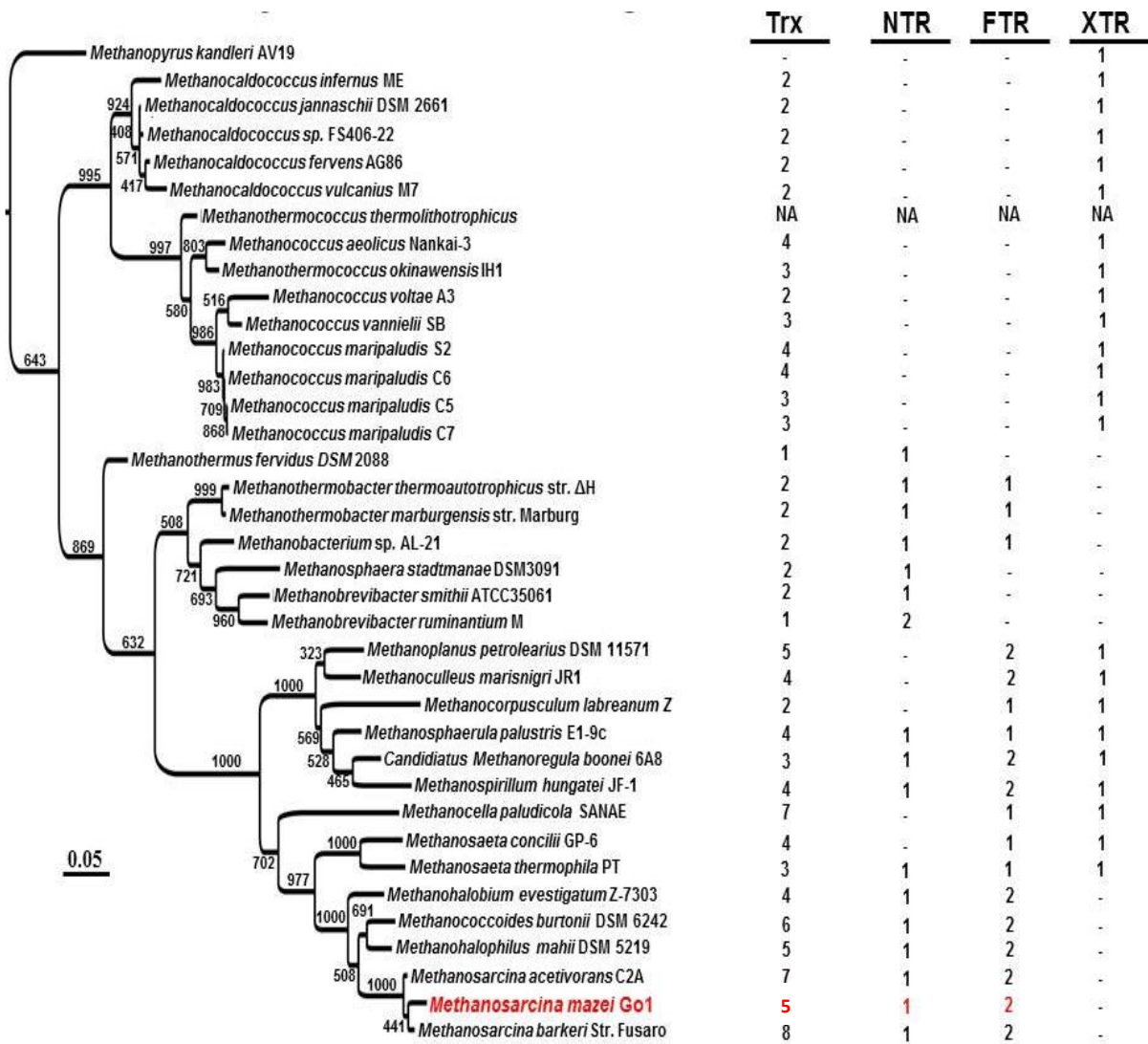


Figure 3. Distribution of Trx, FTR, and NTR in methanogenic archaea. Shown in red are *Methanosarcina mazei* and five Trxs, one NTR, and two FTRs that are present in this organism. This figure is an unpublished data from Dr. Dwi Susanti.

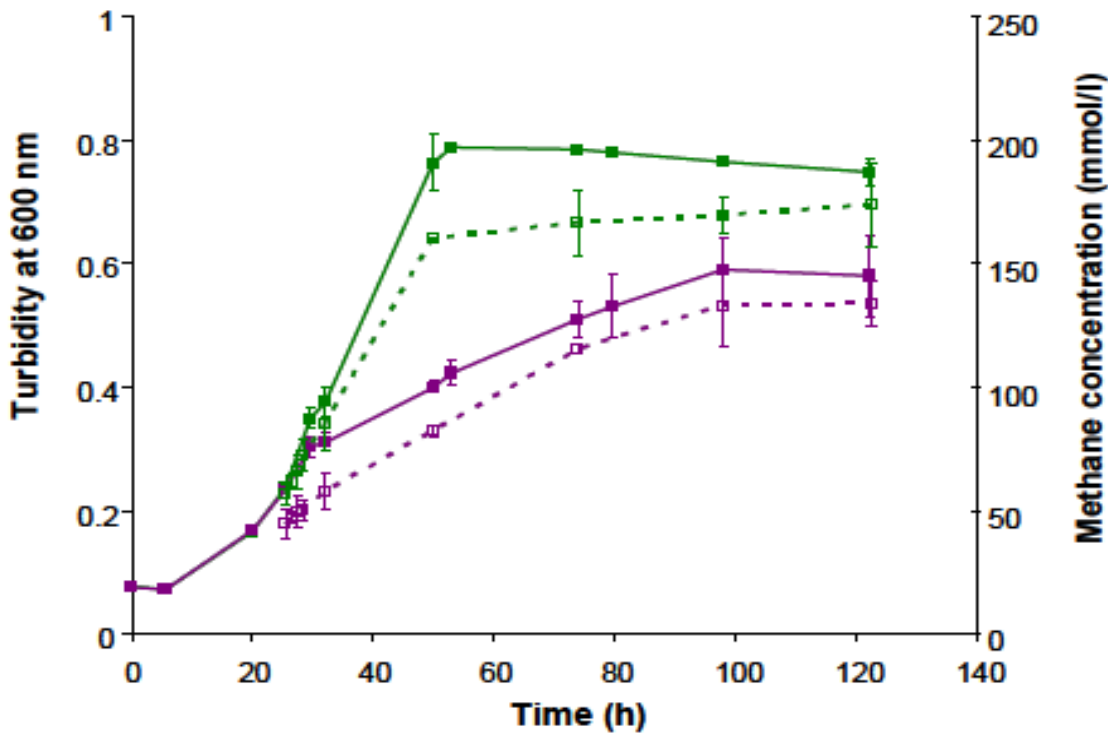


Figure 4. Growth of *Methanosaeca mazaei* under anaerobic and oxygen exposed conditions. *M. mazaei* was grown anaerobically at 37°C with methanol as the methanogenic substrate and carbon source [1]. Growth was followed by measuring the turbidity of the culture at 600 nm. For oxygen stressed conditions, the cultures were grown anaerobically and sterile air (final concentration of oxygen, 4.2%) was introduced into the headspace of the culturing vessel, after 24 h of growth. Methane production was monitored by using gas chromatography. ----- CH₄ produced. _____ Growth. **Green** Anaerobic culture. **Purple** O₂ culture. The data were provided by Schmitz – Streit’s laboratory at the University of Kiel, Germany.

Chapter 2: MATERIALS AND METHODS

Construction of vectors for the expression of *M. mazei* NTR, FTRs, and Trxs in *E. coli*

The construction of expression vectors occurred in two different laboratories. Each was based on the T₇ promoter and designed to generate recombinant proteins with an NH₂ – terminal His₆-tag in *E. coli*. The vectors for the three Trxs (MM_0737, MM_2079, and MM_2249) and the co-expression vector for MM_NTR and MM_Trx5 (using the native intergenic region), were constructed by me in our laboratory. The respective coding sequences were PCR amplified from the chromosomal DNA of *M. mazei* using the primers purchased from IDT Inc. (Coralville, Iowa, USA) as listed in Table 1 and the resulting amplicons were cloned into the *Nde*I and *Bam*H I sites of the expression vector pTev5 [62] to generate the expression plasmids, pUL221, pUL222, pUL223, and pUL224, respectively.

In the case of MM_Trx5 (*mm_2354*), at first a synthetic gene with codons optimized for expression in *E. coli* was obtained from IDT, as an insert in the plasmid pIDTSmartMM_2354. Then the insert was excised with *Nde*I and *Bam*H I and cloned into similarly digested pTev5 to generate the expression plasmid pUL225.

The vectors for MM_Trx1 (MM_0436), NTR (MM_2353) and FTRs (MM_0057 and MM_3270) were constructed in the laboratory of Dr. Ruth Schmitz-Streit at the University of Kiel, Germany. In each case the respective coding sequence was cloned into the expression vector pET28a at the *Nde*I and *Xba*I sites to generate the plasmids pRS697, pRS532, pRS530, and pRS553, respectively.

Expression of *M. mazei* Trxs, NTR, and FTRs in *E. coli*

In each case, the expression host, *E. coli* BL21(DE3)(pRIL), carrying an appropriate expression plasmid and pRIL was grown in LB medium at 37°C. The pTev5 and pET28a based plasmids were selected on 100 µg/mL ampicillin and 20 µg/mL kanamycin, respectively. The plasmid pRIL (Novagene, EMD Millipore Corporation, Billerica, MA, USA) was selected for by using 34 µg/mL chloramphenicol; it helps

to increase the abundances of select arginine, leucine, isoleucine tRNAs that are rare in *E. coli* but commonly used by archaea such as *M. mazei*. The culture was grown up to an optical density of 0.6 as measured at 600nm with a DU800 spectrophotometer (Beckman Coulter, Brea, CA). Then the expression of the cloned gene was induced with the addition of isopropyl- β -D-thiogalactopyranoside (IPTG) (Sigma, St. Louis, MO) to a final concentration of 0.4 mM and the culture was incubated for additional three hours. Finally, the cells were harvested by centrifugation at 10,000 x g and stored in -20°C until used [42].

Purification of the recombinant proteins

Each recombinant protein was purified by Ni²⁺ - affinity chromatography as described previously [42, 63], and following is a brief description of the process. The *E. coli* cells with the over-expressed protein were suspended in a lysis buffer (50 mM sodium phosphate buffer pH 8, 300 mM NaCl, and 10 mM imidazole) and lysed using a French pressure cell operating at 1280 psi pressure; the process involved three passages through the pressure cell. The lysate was centrifuged at 18,000 x g, at 4°C for 30 minutes. The resulting supernatant was then loaded onto a Ni-NTA column (equilibrated with the lysis buffer containing 10 mM imidazole), and after a wash with 5 volumes of the lysis buffer (with 10 mM imidazole), the proteins were eluted with solutions containing 50 mM sodium phosphate buffer pH 8, 300 mM NaCl and imidazole at concentrations ranging from 50 mM to 300 mM. The fractions were collected as 2 mL portions on ice, and examined via SDS-PAGE to determine their compositions in terms of the number of polypeptides present therein. The fractions containing the desired protein in apparent homogeneous form, were pooled together and concentrated using Amicon 3K centrifugation filters (EMD Millipore Corporation, Billerica, MA, USA) at 4°C. The protein concentration in this solution was determined via Bradford's Coomassie Blue assay [64].

Table 1. List of primers used for amplifying Trx and TrxR coding sequences

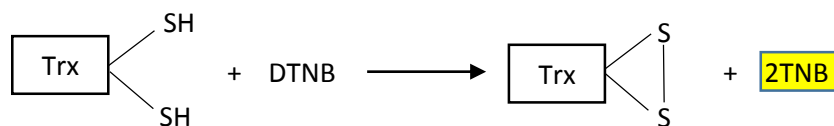
Gene	Primer	Sequence (restriction sites underlined)	Restriction Site
<i>mm_0706</i>	MM_0706Nde/F	AAA <u>ACATATGAGTCATAAATGTTTAAGG</u>	<i>Ndel</i> CA [^] TA _^ TG
	MM_0706Bam/R	AGA <u>AGGATCCTTAATCTCCTCCGAGGGGC</u>	<i>BamHI</i> G [^] GATC _^ C
<i>mm_0737</i>	MM_0737/F	GCT <u>CAGCATATGAAATACATGAAAATCG</u>	<i>Ndel</i> CA [^] TA _^ TG
	MM_0737/R	GC <u>AGGATCCTCATTGGTGATCCAT</u>	<i>BamHI</i> G [^] GATC _^ C
<i>mm_2079</i>	MM_2079Nde/F	AGT <u>TGCATATGAACGGAAGCAGTATAATCG</u>	<i>Ndel</i> CA [^] TA _^ TG
	MM_2079Bam/R	AT <u>GAAGGATCCTTATACGTATCCTGTAATG</u>	<i>BamHI</i> G [^] GATC _^ C
<i>mm_2249</i>	MM_2249/F	GCT <u>CAGCATATGAAAATAGAAATTCTCG</u>	<i>Ndel</i> CA [^] TA _^ TG
	MM_2249/R	GC <u>AGGATCCTTAGATCATCCATTT</u>	<i>BamHI</i> G [^] GATC _^ C
<i>mm_2354</i>	pTev5Ncol/F	CAT <u>CCATGGCGTACTACCAC</u>	<i>Ncol</i> C [^] CATG _^ G
	MM_2354BgIII/R	CT <u>GGAGATCTCATGTAATACGGGC</u>	<i>Bg</i> III A [^] GATC _^ T
<i>mm_2353-4</i>	MM_2354/F	CT <u>TCAGCATATGTTTTAGAATTACAGATT</u> C	<i>Ndel</i> CA [^] TA _^ TG
	MM_2353Bam/2R	CAGT <u>GGATCCTCATCTAATTTCTCAA</u>	<i>BamHI</i> G [^] GATC _^ C
<i>mm_2353-4</i>	MM2353-4mRNA/1F	GCC <u>CAGGAAGGACAGGCCCTAATTG</u>	
	MM2353-4mRNA/2R	CCATT <u>GAGATCTGGCCGCTG</u>	

Western blot

Western blot analysis, to detect the presence of *E. coli* Trx and NTR in the purified preparations of recombinant Trxs and NTR of *M. mazei*, was carried out as described previously [65]. *E. coli* NTR and Trx were used as positive controls. Here I describe only the steps that are specific to this study. The membrane carrying the blotted proteins were blocked with 5% skim milk, by immersing it in the blocking solution and gently agitating overnight at 4°C. Primary rabbit antisera raised against *E. coli* Trx and NTR, (a gift of Dr. B. B. Buchanan, University of California, Berkeley, CA) were used at a dilution of 1:3000. Anti-rabbit IgG (whole molecule) alkaline phosphatase conjugate (Sigma, St. Louis, MO) was used as the secondary antibody, at a dilution of 1:5000. The membrane was developed with nitro blue tetrazolium and 5-bromo-4-chloro-3-indolyl phosphate (Sigma, St. Louis, MO), to visualize the antisera reacting bands.

State of oxidation of *M. mazei* Trxs

Purified recombinant proteins of *M. mazei* Trxs were examined for their states of oxidation by their ability to reduce 5,5'-Dithiobis(2-nitrobenzoic acid) (DTNB). For this assay a reaction mixture of the following composition was added to a spectrophotometer cuvette: 1 mM EDTA, 100mM potassium phosphate buffer (pH 7), and 2 µM Trx in a final volume of 600 µL. Then DTNB (TCI America, Portland, OR, USA) was added to the mixture to a final concentration of 0.2 mM and its reduction was observed by a rise in absorbance at 412 nm using a Beckman DU800 spectrophotometer. This assay detects reduced Trx via the following reaction.



Oxidation and reduction of *M. mazei* Trxs

This experiment was performed to determine if the reduced Trx can be oxidized chemically and the oxidized Trx obtained from this reaction can be re-reduced. If this were possible, it would allow us to generate biologically active forms of oxidized Trx for NTR assays. The following steps were carried out as described previously in my publication but with some modifications [42].

A Trx was oxidized by incubating at room temperature for 2 hrs in the following reaction mixture in a final volume of 1 mL: 20 mM potassium phosphate buffer (pH 7), 100 µM DTNB and 10 µM of Trx. The free thiols, if present in this oxidized Trx preparation, were blocked by the addition of iodoacetamide (IAA) and N-ethylmaleimide (NEM), each at a final concentration of 100 µM followed by incubation at room temperature for 20 min. The blocking reaction was stopped with the addition of β-mercaptoethanol (βME, final concentration, 10 µM). The reaction mixture (1 mL) was dialyzed overnight against 1 L of 25 mM potassium phosphate buffer, pH 7, with 10% (w/v) glycerol, at 4°C with three changes of buffer. The oxidized Trx was reduced by incubation with DTT (final concentration, 1 mM), on ice for 30 min.

Analysis of oxidized and re-reduced Trx preparations

Three preparations were analyzed: Trx as purified, Trx oxidized with DTNB, and oxidized Trx re-reduced with DTT. 500 µL of each preparation was incubated with the fluorescence probe monobromobimane (mBBr), at a final concentration of 1 mM in the dark and on ice for 30 min. Then βME was added (final concentration, 10 mM) to quench excess mBBr, and the protein was precipitated by adding equal volume of 20% ice cold trichloroacetic acid (TCA) (Sigma, St. Louis, MO) to the solution and incubating the mixture on ice for 20 min. After recovery by centrifugation (16,000 x g), the protein pellet was washed with an equal volume of ice cold acetone, air dried for 1 min, and dissolved in distilled water. The Trx solution was subjected to SDS-PAGE, and then the fluorescent band of mBBr labelled Trx was viewed under 635 nm UV light.

Insulin Reduction Assay for Trxs

Insulin reduction assay (Figure 5) was performed in triplicate for each of the Trxs as described previously [35, 42], at 37°C. A 600 µL reaction mixture of the following composition was added to a cuvette: 100mM potassium phosphate buffer (pH 7), 2 mM EDTA, 0.087 µM bovine insulin (Sigma, St. Louis, MO), and 2 µM Trx. Then the assay was initiated by the addition of the electron donor, DTT (final concentration, 1 mM), and insulin precipitation was observed by the increase in optical density at 650 nm using a Beckman DU800 spectrophotometer.

Growth of *Methanosarcina mazei*

Methanosarcina mazei was grown as previously described using methanol as the methanogenic substrate [1, 66]. Each 50 mL culture was grown anaerobically in a sealed 160 mL serum bottle at 37°C. Cells were harvested aerobically at the log phase (OD_{600} 0.3) via centrifugation at 10,000 x g, frozen immediately in liquid nitrogen and stored at -80°C until used for RNA extraction.

RT-PCR of *ntr* (*mm_2353*) and *trx* (*mm_2354*) mRNA

Total mRNA from *M. mazei* cells was isolated and converted to cDNA by reverse transcription, using RNeasy mini kit from QIAGEN (QIAGEN Inc., Valencia, CA 91355) [66]. Then PCR was performed using primers MM_2353-4mRNA/1F and MM_2353-4mRNA/2R (Table 1), which helps to amplify parts of *mm_2353* and *mm_2354* genes along with the inter-genic region. Three PCR reactions were performed using the following templates: total RNA as negative control, gDNA as positive control, and the cDNA as the test sample. The amplification products were examined by agarose gel electrophoresis. The expected size of the PCR product was 305 bp.

Amino acid sequence alignment

The amino acid sequences of five thioredoxins of *M. mazei*, *E. coli* Trx, and Trxs of *M. jannaschii*, MJ_0307 and MJ_0581, were compared using Clustal Omega [67]. Similarly, MM_NTR was compared with

the NTRs from *E. coli* and *M. jannaschii*. A comparison was performed for the FTRs of *M. acetivoranse* (MA2870 and MA1659), *M. barkeri* (Mbar_A2920 and Mbar_A2432) and *M. mazei* (MM_0057 and MM_3270) as well.

Reconstitution of MM_NTR with Flavin Adenine Dinucleotide (FAD)

Purified MM_NTR was reconstituted with FAD (Sigma, St. Louis, MO) as previously described [63], by incubating 45 µg of MM_NTR with FAD (concentration, 1 mM above that of NTR) in a 1 mL solution containing 20 mM potassium phosphate buffer pH 7, on ice for one hour. The unbound FAD was removed by washing the protein three times with 20 mM potassium phosphate buffer (pH 7), on a 3K Amicon filter (EMD Millipore Corporation, Billerica, MA, USA), under centrifugation at 7000 x g, at 4°C. The protein concentration in the solution of the reconstituted MM_NTR was determined via Bradford assay [64] using BSA as the standard.

UV visible spectroscopy with NTR and FTR

UV visible spectra for the purified recombinant NTR (before and after reconstituting with FAD), FTR1 and FTR2 were obtained in the 200 – 600 nm range using a Beckman DU800 spectrophotometer. The analysis was performed in a quartz cuvette with a solution of a Trx reductase in 20 mM potassium phosphate buffer (pH 7).

DTNB Reduction Assay for NTR

The DTNB reduction assay for NTR (Figure 6) was performed as described previously [68], at 37°C, by using a reaction mixture of the following composition: 100mM potassium phosphate buffer (pH 7), 50 nM NTR, 1 mM EDTA, 0.2 mM NADPH (the electron donor) (Sigma, St. Louis, MO), and 0.2 mM DTNB, in a total volume of 600 µL. The increase in absorbance at 412 nm due to the reduction of DTNB to NTB, was followed using a Beckman DU800 spectrophotometer.

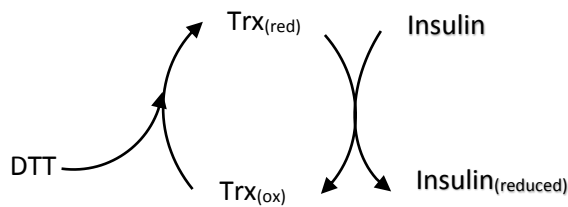


Figure 5. Insulin reduction by Trx with DTT as electron donor. Schematic representation of the assay. The insulin precipitation is observed spectrophotometrically at 650 nm.

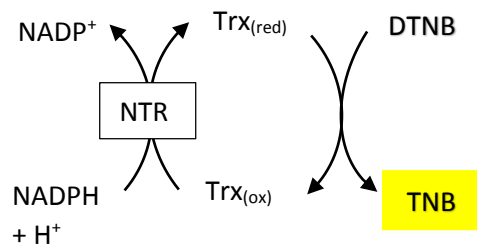


Figure 6. DTNB reduction assay for NTR. NADPH is the primary electron donor. The reduction of DTNB is observed spectrophotometrically at 415 nm (yellow color).

FTR assays:

Insulin reduction assay with dithionite as the electron donor

The assay (Figure 7) was conducted under anaerobic conditions at 37°C [59], with an assay mixture of the following composition: 100 mM potassium phosphate buffer (pH 7), 2 mM EDTA, 0.5 mg/mL bovine insulin, 50 nM FTR, 2 µM Trx, and 2.5 mM dithionite (Sigma, St. Louis, MO), in a total volume of 600 µL. The reaction was initiated by the addition of dithionite and insulin precipitation was recorded at 650 nm using a Beckman DU800 spectrophotometer.

Insulin reduction assay with clostridial ferredoxin and hydrogenase for electron delivery

The procedure is similar to that described in the preceding section except for the following. Ferredoxin reduced with H₂ gas and hydrogenase was used as electron donor; the ferredoxin and hydrogenase were purified from *Clostridium pasteurianum*, (a gift from Dr. Jiann-Shin Chen, Virginia Tech, Blacksburg) (Figure 9) [69]. The assay mixture had the following composition: 60mM Tris-Cl (pH 8), 0.5 mg/mL insulin, 1 µM clostridial hydrogenase, 5 µM clostridial ferredoxin, 1 µM FTR, and 10 µM Trx, in a total volume of 600 µL. It was made anaerobic by alternate cycles of vacuum and pressurization with N₂ gas, and finally N₂ was replaced with H₂ at a pressure of 5 psi [63]. The reaction was initiated by the addition of clostridial ferredoxin.

DTNB assay for FTR2 with spinach FNR and NADPH for electron delivery

This assay was exclusively performed for FTR2, with the aim of reducing the C-terminal rubredoxin unit by ferredoxin NADPH oxidoreductase (FNR) (a gift from Dr. Bob B. Buchanan, University of California, Berkeley) with NADPH as the primary electron donor (Figure 10) [33]. The assay was performed aerobically at 37°C, and had the following composition: 100mM potassium phosphate buffer (pH 7), 0.2 mM DTNB, 0.2 µM spinach FNR, 0.2 mM NADPH, 100 nM FTR2, 2 µM Trx, in a total volume of 600 µL. The reduction

of DTNB was monitored spectrophotometrically at 412 nm. The reaction was initiated by the addition of NADPH.

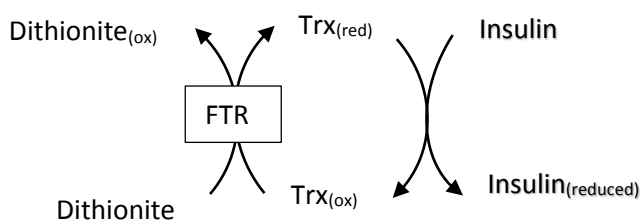


Figure 7. Insulin reduction assay for FTR. Dithionite is the primary electron donor. The reduction of insulin is observed spectrophotometrically at 650 nm.

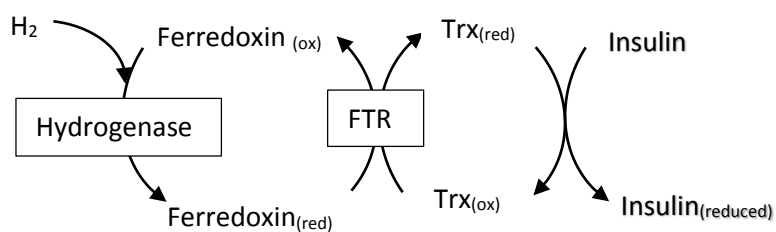


Figure 8. Insulin reduction assay for FTR. Ferredoxin reduction was catalyzed by a hydrogenase from *Clostridium pasteurianum*. The reduction of insulin was observed spectrophotometrically at 650 nm.

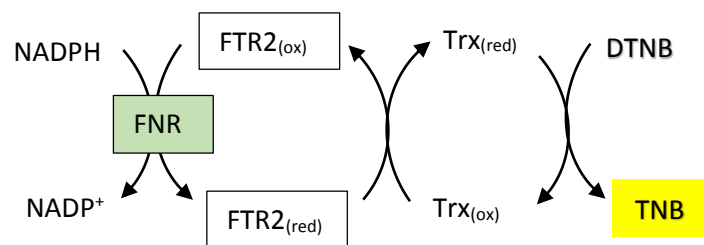


Figure 9. DTNB reduction assay for FTR2. NADPH is the primary electron donor for the reduction of the C – terminal rubredoxin domain of FTR2, and the reaction is catalyzed by spinach ferredoxin NADPH oxidoreductase (FNR). The reduction of DTNB is observed spectrophotometrically at 415 nm.

Chapter 3: RESULTS

Structural and functional characteristics of the thioredoxins and thioredoxin reductases of *M. mazei*

Primary structure characteristics of the thioredoxins of *M. mazei*

The five thioredoxin (Trx) homologs of *Methanosarcina mazei*, *mm_0436*, *mm_0737*, *mm_2079*, *mm_2249*, and *mm_2354*, (named as MM_Trx1-5, respectively in this study), were identified via BLAST search using *E. coli* and *Methanocaldococcus jannaschii* Trxs as queries. A comparison of the amino acid sequences of these proteins and the Trxs of *M. mazei* MM_0436, MM_0737, MM_2079, MM_2249, and MM_2354 is shown in (Figure 10). The redox active site motifs of MM_Trx1 – 5 are CGPC, CAKC, CPYC, CPKC, and CTAC respectively. MM_Trx1 has the same active site motif of CGPC, as the *E. coli* Trx (EcTrx), MM_Trx4 motif is the same as that of MjTrx2, while MM_Trx3 has an active site motif (CPYC) which is typical for glutaredoxin. In amino acid sequences the five *M. mazei* Trx homologs showed > 20% identities and > 40% similarities with the *E. coli* Trx; MM_Trx1 showed the highest identity and similarity (39% and 57%, respectively). When compared to the Trx homologs of *M. jannaschii*, they showed > 30% identities and > 50% similarities to MjTrx1, with MM_Trx4 having the highest identity and similarity values (39% and 57% respectively). MM_Trx2 showed the highest identity and similarity (54% and 71% respectively) to MjTrx2, whereas MM_Trx3, MM_Trx4, and MMTrx5 showed identity between 26 to 39% and similarity between 41 and 67%, while MM_Trx1 did not show significant similarity to MjTrx2.

Primary structure characteristics of NADPH thioredoxin reductase (NTR) of *M. mazei*

The NTR (MM_NTR) of *M. mazei* has a conserved FAD binding domain, and is comprised of an N-terminal GGGPAG and a C-terminal GIYAAGD elements. The NADPH binding domain GGGNSA occurs in the middle of the sequence, and the enzyme has an active site motif of CAIC (Figure 11) [70]. When compared with NTRs of other *Methanosarcina* species, MM_NTR (MM_2353) showed higher aminoacid

sequence identity and similarity to *Methanosarcina acetivorans* NTR MA1368 (83% and 92%, respectively), than to *Methanosarcina barkeri* Mbar_A2898 (76% and 88% respectively). It exhibited lower identity and similarity to the well-studied *E. coli* NTR (37% and 57% respectively). The MM_2353 protein had 32% identity and 51% similarity to *Clostridium acetobutylicum* NTR CA_C1548, and it was also similarly related to the thioredoxin reductase (MJ_1536) of the deeply rooted methanogenic archaeon *M. jannaschii* (41% identity and 59% similarity).

Primary structure characteristics of ferredoxin thioredoxin reductases (FTR) of *M. mazei*

The two ferredoxin thioredoxin reductases of *M. mazei*, FTR1 (MM_0057) and FTR2 (MM_3270), belong to Group IV and Group VI FTRs, respectively. FTR1 has the catalytic site sequence of CPCRIVTGDESEDKKIVCPCVYHKDEIEKDGNCHC with the conserved motif of CPCX14CPCX12CHC, which represents Group IV (Figure 12) [54]. The FTR2 catalytic site sequence of CPCRLSADNKEEDLDIICPCYYRDPDLNDYGACYC represents the conserved sequence motif of CPCX14CPCX12CYC of Group VI [54]. It also has a rubredoxin domain fused to the C-terminus as found in some members of the Group VI FTRs (Figure 13). The amino acid sequences of *M. mazei* FTRs were also compared to respective homologs in other *Methanosarcina* species. The values for the identities and similarities of FTR1 (MM_0057) to the other FTRs were as follows: *M. acetivorans* (MA2870), 92% and 98%; *M. barkeri* (Mbar_A2920), 77% and 93%. The corresponding values for the identities and similarities of FTR2 (MM_3270) were as follows: *M. barkeri* (Mbar_A2432), 87% and 94%; *M. acetivorans* (MA1659), 85% and 92%.

MJ_0581	-----
MM_0737	-----
MM_2249	-----
MM_2354	-----MFLELQIRSTYLYLEINNRNGNLYNLSFWR
MJ_0307	-----
MM_2079	-----MNGSSIIIEFE-----DMTWS-QQVE
EcTrxA	-----MSDKIILHT-----DDSFDTDVL
MM_0436	-----
 MJ_0581	MVRVMVVIRIFGTGCPKCNQTYENVKKAVEELGIDAEIVKVT---DVNEIAEW-VFVTPG
MM_0737	--MKYMKIEILGTGCAKCKKTAKELAEKAVKELGVDAEIVKVE---DFDKILGYGVMVTPA
MM_2249	-----MKIEILGTGCPKCKKTAKETIEKVLKQTGVEAEVIKVE---DIEKIMSYGVMVTPA
MM_2354	YLSTVKVTLIHATWCTACPATRRLFVNLDLKSVDYDFEYEEIDVESSEQQALIDKYGIVGVPT
MJ_0307	-MSKVKIELFTSPMCPHCPAAKRVVEEVANEMPDAVEVEYINVMPNPKAMEYGIMAVPT
MM_2079	DSKKPVVVMFYSPACPYPCKAMEPYFEYAKEYGGSAVGRNIAATNPWTAEKYGVQGTPPT
EcTrxA	KADGAILVDFWAECGHCKMIAPIDEIADEYQGKLTVAKLNDQNPGBTAPKYGIRGIPPT
MM_0436	--MKPMLLDTSATWCGHCRMQKPILEELKKYGDVKVVDVDEQELASKYGIHAVPT
	: . * * .. : : : : * :
 MJ_0581	VAFDDVI---VFEGKIPSVEEIKEELKSYLEGK-----
MM_0737	LVIDGDV---KVAGKVPSPVEDIKKWITK-----
MM_2249	VVIDGEV---KLAGKVPDEKDVRKWM-----
MM_2354	TLIDGEPE---AFTGL-PKKAFAAIARIT-----
MJ_0307	IVINGDV---EFIGA-PTKEALVEAIKKRL-----
MM_2079	FKFFCHGRPVWEQVGO-IYPSILKNAVDRMLQHGEECIRKSTPGQDITGYV
EcTrxA	LLLFKNGEVAATKVGA-LSKGQLKEFLDANLA-----
MM_0436	LTIQKDGTEVKRFMGV-TQGSVLAAELDKLL-----
	: * : :

Figure 10. Multiple sequence alignment of the thioredoxins (Trxs) of *Methanosarcina mazei*, *Escherichia coli*, and *Methanocaldococcus jannaschii*. EcTrxA, *E. coli* thioredoxin; MJ_0307 and MJ_0581, *M. jannaschii* Trx1 and Trx2; MM_0436, MM_0737, MM_2079, MM_2249, and MM_2354, *M. mazei* thioredoxins MM_Trx1-5. The sequence alignment was performed using Clustal Omega [67]. The conserved amino acid residues are marked with *. The active site cysteines are enclosed in boxes.

EcTrxB MM_2353 MJ_1536	MGTTKHSKLLIIGSGPAGYTAAVYAARANLQPVLITGMEKGQLTTTEVENWPGDPNDL -----MYDLIIIGGGPAGLTAGIYAVRYGLDTLILERNEISGQISMADIVENYPGFPSS-I ----MIHDTIII[GAGPGGLTAGIYAMRGKLNALCIEKENAGGRGIAEAGIVENYPGFEI-I . : * : * . * * . * * . : * * : * : : . : . * : : : * * : * * . :
EcTrxB MM_2353 MJ_1536	TGPLLMERMHEATKFETEIIFDHINKVDLQNRPFRLNGDNGEYTCDALIATGASARYL SGLELMERFRTHAQEVGVKTITEVLSVRSEGKKIITTDGDEAKAVIATGANPKHL RGYELAEKFKNHAEKFKLPIIYDEVIKETKERPFKVITKNSEYLTKTIVIATGTPKKL . * * * : : * * : .. . : . : : : . . : . : . : * : * : * : * :
EcTrxB MM_2353 MJ_1536	GLPSEEAFKGRGVSA[CATCDGFFYRNQKVAVI[GGGNTA/VEEALYLNSNIASEVHLIHRRDG GVPGEKELISKGVSYCAICDGPFFRNKIVAVV[GGGNSAVTDALFLSKVAQKVYLHRRDH GLNE-DKFIGRGSISYCTMCDAFFYLNKEVIVI[GPDTPAAMSAINLKDIAKKVIVITDKSE . : . : . : * : * : * * : * : * : * : * : * : * : * : * : * : * : ..
EcTrxB MM_2353 MJ_1536	FRAEKILIKRMLDKVENGNIILHTNRTLEEVTGDQMGTGV--RLRDTQNSDNIESLDVA LKAA-RVLQDRVDGTPNIELILN--SHVLEIVGTRREGIKKVEKIILEDVNSRETRELSTN LKAAESIMLDKLKEANNVEIYNN--AKPLEIVGEEERAEGVK--I--SV-NGKEEIKAD . : * : : . : . . * : * : . * : . * : . . : . : . : . . :
EcTrxB MM_2353 MJ_1536	GLFVAIGHSPNTAIFEGQ--LELENGYIKVQSGIHGNATQTSI[HGVFAAGDMDHIYRQA GVFIYVGIHPNTEFVD--VEKDEGGFIKTDR----WMETSEKGIYAAGDCRDTPIWLQ GIFISLGHVPNTEFLKDGSIELDKKGFIKTDE----NCRTNII[CIVAVCDVRGG-VMQV . : * : * *** : . : * : * : . : * . * : * : * : * : * : * : * : * : *
EcTrxB MM_2353 MJ_1536	ITSAGTGCMAALDAERYLDGLADAK VTAVRDGAIAATAAYEYIEKIR--- AKAVGDGCVAMANIICKYLQKL--- . . . * : * . * : :

Figure 11. Multiple sequence alignment of NADPH thioredoxin reductase (NTR) from *Methanosa*cina *mazei*, *Escherichia coli*, and *Methanocaldococcus jannaschii*. The conserved amino acids are marked with the *. The sequences in blue boxes represent the FAD binding domain. The NADPH binding domain sequences are boxed in red [70].

Figure 12. Multiple sequence alignment of ferredoxin thioredoxin reductase-1 (FTR1) of *Methanosarcina mazei*, and respective homologs in *Methanosarcina acetivorans*, and *Methanosarcina barkeri*. FTR1 is a group IV FTR with the active site motif of CPCX₁₄CPCX₁₂CHC. The conserved CPC and CHC elements that provide the cysteine residues for forming the Fe-S cluster are boxed [54].

Figure 13. Multiple sequence alignment of ferredoxin thioredoxin reductases-2 (FTR2) of *Methanosarcina mazei*, *Methanosarcina acetivorans*, and *Methanosarcina barkeri*. FTR2 is a group VI FTR with a catalytic site motif of CPCX₁₄CPCX₁₂CYC. The boxed CPC and CYC elements harbor the cysteine residues that form the Fe-S cluster. Conserved amino acids are indicated by *. The conserved sequences of the C-terminal rubredoxin domain are boxed in red [54].

Experimentally determined characteristics of the Trxs and TrxRs of *M. mazei*

The genes encoding for MM_Trx1-4 are monocistronic, while the gene *mm_2354* encoding for MM_Trx5 forms an operon type arrangement with the upstream gene *mm_2353* that encodes an NTR (Figure 14). RT-PCR targeting parts of *mm_2353* and *mm_2354* along with the inter-genic region resulted in a PCR product of about 300 bp, which indicated that these genes were indeed co-transcribed, and therefore belong to an operon. (Figure 15).

Each of the Trx proteins (MM_Trx1-4), the NTR and FTR1 & FTR2 of *M. mazei* were overexpressed successfully in soluble forms in *E. coli* BL21(DE3)(pRIL) (Figure 16-22). MM_Trx5 was not over-expressed in this *E. coli* strain even after induction with lower concentrations of IPTG and at 15°C. The co-expression of MM_Trx5 with MM_NTR from a single expression vector resulted in high expression of MM_NTR, but very low amounts of MM_Trx5 (data not shown). When the codons of *mm_trx5* were optimized for its expression in *E. coli*, the protein was expressed in a soluble form and at a workable level in *E. coli* BL21(DE3) (Figure 23).

The Trx and TrxR proteins were purified using Ni²⁺ affinity chromatography [42]. The data from SDS - PAGE analysis for the cell extracts and the column fractions of these proteins eluted from the column with various concentrations of imidazole are shown in (Figure 24-31). Following the purification, all five recombinant thioredoxins and the NTR preparations were analyzed via Western blot using antisera raised against *E. coli* Trx and NTR; FTR preparations were not analyzed since *E. coli* does not possess an FTR gene. The results showed that the purified recombinant *M. mazei* proteins were free of the *E. coli* homologs.

The recombinant NTR of *M. mazei* as purified was yellow in color, indicating the presence of the cofactor flavin. Considering that some of the molecules might have lost flavin, the preparation was reconstituted with added FAD. UV-visible spectroscopic analysis of the purified protein, before and after reconstituting with FAD, showed absorbance peaks at 375 nm and 450 nm, which are typical of a flavin

cofactor (Figure 32). The reconstituted protein exhibited 75 fold higher $A_{450}/\mu M$ value (Figure 32) than the purified preparation, indicating substantial loss of bound flavin during purification. Such a loss is common for flavo proteins [63].

The purified preparations of two FTRs were brown in color, which is an indication for the presence of Fe-S clusters in these proteins as their cofactor. UV-visible spectra showed absorbance maxima at 340 nm and 410 nm for FTR1 and 345 nm and 415 nm for FTR2, and these observations further supported the presence of Fe-S clusters (Figure 33).

Oxidation and reduction of Trxs

The purified preparations of MM_Trx1, and MM_Trx5 were always in their reduced forms, as they reduced DTNB without the aid of a reductant and a thioredoxin reductase, whereas MM_Trx2, MM_Trx3, and MM_Trx4 were sometimes in oxidized forms as they were unable to reduce DTNB. Also, reaction with mBBr did not yield fluorescent bands for MM_Trx2 and MM_Trx4, but did in case of MM_Trx1, MM_Trx3 and MM_Trx5 in SDS – PAGE analysis. These results further validated the conclusion that the purified preparations of MM_Trx2 and MM_Trx4 were in oxidized states and MM_Trx1, MM_Trx3, and MM_Trx5 were in reduced states.

The reduced forms of the MM_Trx1 and MM_Trx3 were successfully oxidized with excess DTNB. When oxidized Trxs were treated with the fluorescent probe mBBr and then analyzed via SDS – PAGE, these proteins did not exhibit fluorescence under UV light; this was due to the absence of any free thiols in the proteins. When an oxidized Trx was reduced with DTT and then treated with mBBr they exhibited fluorescent bands (Figure 34).

Insulin disulfide reducing activities of Trxs with DTT as electron donor

Purified recombinant thioredoxins were examined for their disulfide reducing abilities by performing the insulin reduction assays (Figure 35-36). The rate of insulin reduction is defined as a change

in absorbance at 650 nm per min. With 1 mM DTT, MM_Trx1 had the best insulin reducing ability exhibiting an average rate of 0.17 min^{-1} at 37°C , and a lag time of 3 min. MM_Trx5 reduced insulin at a rate of 0.072 min^{-1} with a lag time of 3 min, while the MM_Trxs2, MM_Trx3, and MM_Trx4 were unable to reduce insulin and the respective lag times were 13, 13, and 14 min. The average insulin reduction rate and lag time with DTT alone were 0.02 min^{-1} , and 13 min, respectively.

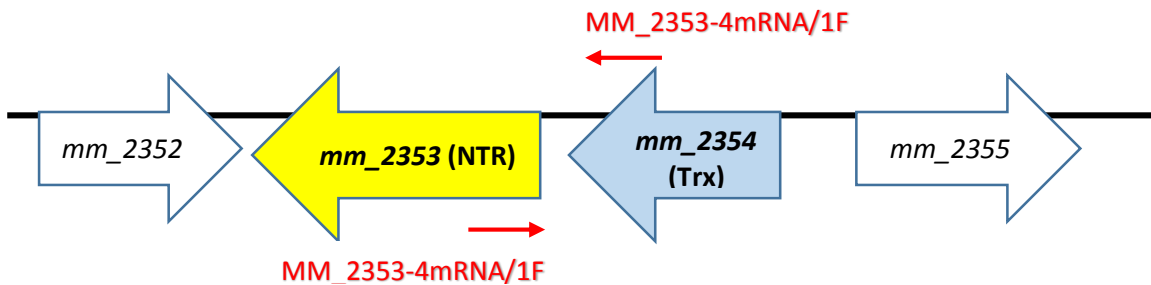


Figure 14. Schematic representation of the operon type gene arrangement of *mm_2353 (ntr)* and *mm_2354 (mm_trx5)* of *Methanomicrobium mazei*. The red arrows represent the primers (MM_2353-4mRNA/1F and MM_2353-4mRNA/2R listed in Table 1) that were designed to amplify the *mm_2353-54* junction region.

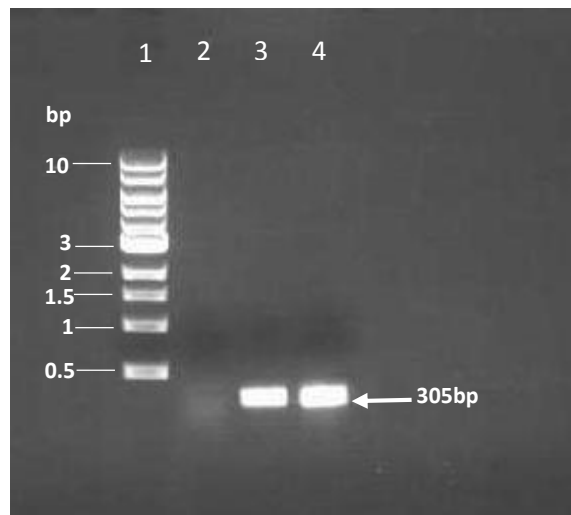


Figure 15. RT-PCR analysis of *mm_2353 (ntr)* and *mm_2354 (mm_trx5)* mRNA targeting the respective junction. The picture is for an agarose gel with ethidium bromide stained PCR products visualized under UV (350 nm). Lane 1: 1 kb DNA ladder. The numbers to the left of the gel indicate the size of each band of the DNA ladder in base pairs (bp). Lane 2: Negative control, PCR done with total RNA of *M. mazei* as the template. Lane 3: PCR using cDNA generated from a total *M. mazei* RNA preparation as the template. Lane 4: Positive control, PCR using *M. mazei* chromosomal DNA as the template. All three PCRs were performed using the primers MM_2353-4mRNA/1F and MM_2353-4mRNA/2R listed in Table 1 and shown in the sketch in Figure 14.

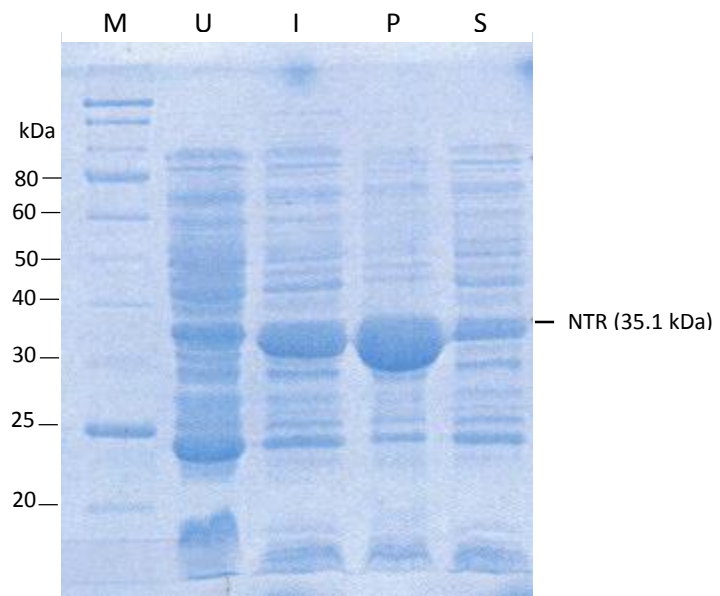


Figure 16. Expression of *M. mazei* NTR (MM_2353) in *E. coli*. SDS-PAGE analysis of cell extracts of *E. coli* BL21(DE3)(pRIL)(pRS532), a strain expressing recombinant MM_NTR. Numbers to the left of the gel picture show the molecular masses of the standards or markers in kDa. The location of the over-expressed NTR band is shown on the right of the picture. M, marker. U and I, extracts of cells where protein expression was not induced or induced with IPTG. P and S, pellet and supernatant from centrifugation (13000 x g) of cell extracts prepared by sonication.

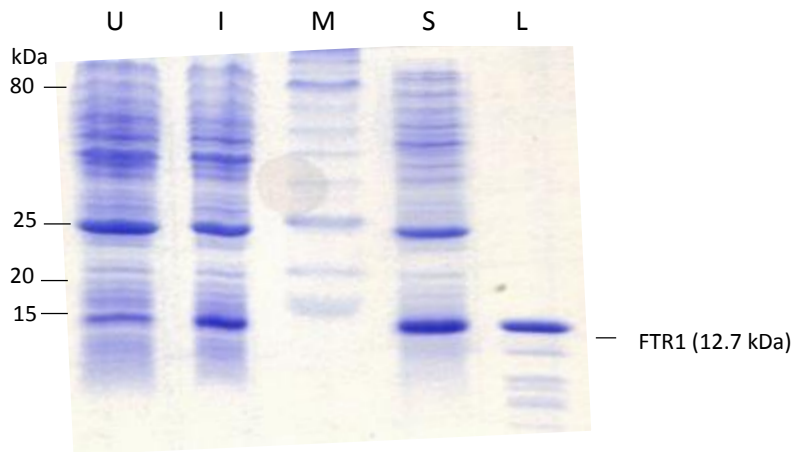


Figure 17. Expression of *M. mazei* FTR1 (MM_0057) and its solubility in *E. coli*. SDS-PAGE analysis of cell extracts of *E. coli* BL21(DE3)(pRIL)(pRS530), a strain expressing recombinant FTR1. Details of this gel picture is the same as in Figure 17, except the cells were lysed using lysozyme and the lysate was centrifuged at 10000xg to separate the supernatant. L, lysozyme used for lysing the cells (14.3 kDa).

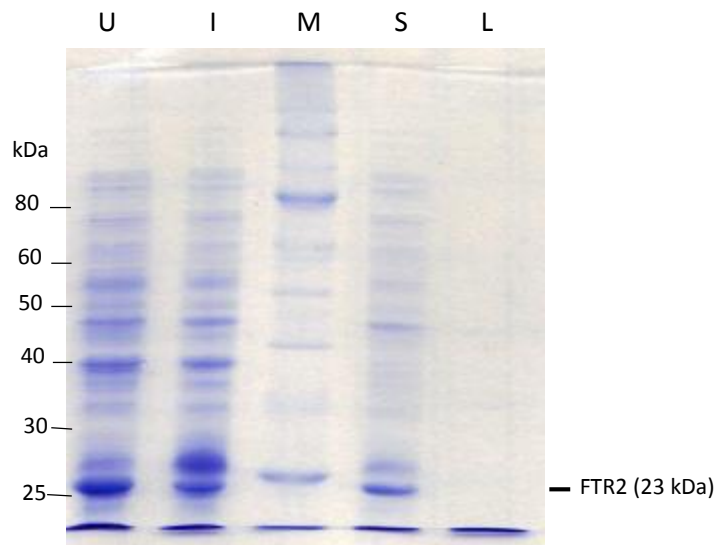


Figure 18. Expression of *M. mazei* FTR2 (MM_3270) and its solubility in *E. coli*. SDS-PAGE analysis of cell extracts of *E. coli* BL21(DE3)(pRIL)(pRS553), a strain expressing recombinant FTR2. Details of this figure is the same as those described in the previous figures 16 - 17.

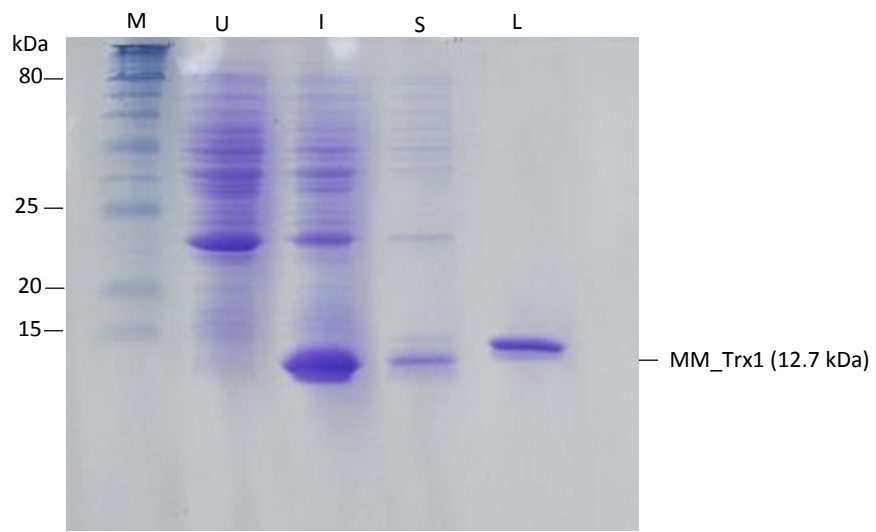


Figure 19. Expression of *M. mazei* MM_Trx1 (MM_0436) and its solubility in *E. coli*. SDS-PAGE analysis of cell extracts of *E. coli* BL21(DE3)(pRIL)(pRS697), a strain expressing recombinant MM_Trx1. Details of the figure are the same as those described previously in Figure 17.

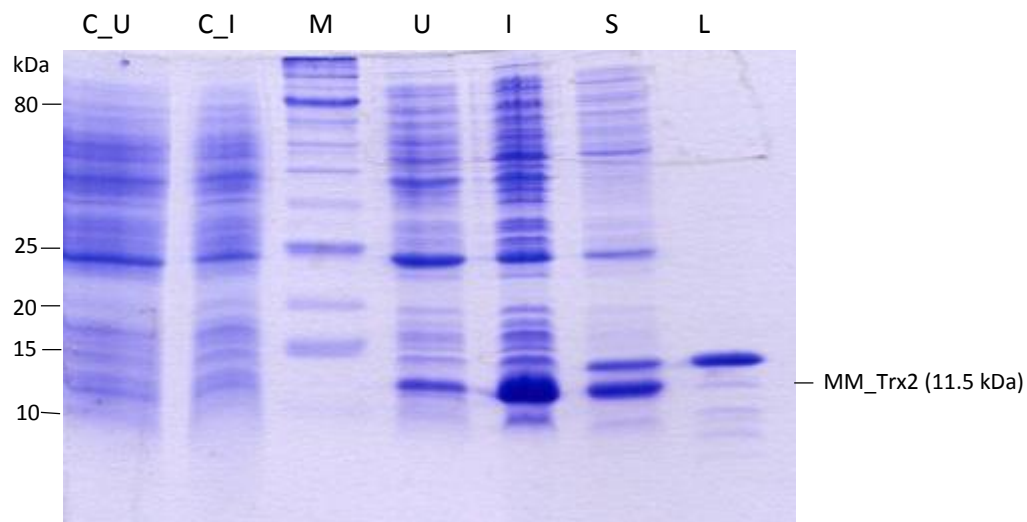


Figure 20. Expression of *M. mazei* MM_Trx2 (MM_0737) and its solubility in *E. coli*. SDS-PAGE analysis of cell extracts of *E. coli* strains: BL21(DE3)(pRIL)(pTev5), vector control; BL21(DE3)(pRIL)(pUL221), a strain expressing recombinant MM_Trx2. C_U, and C_I, extracts of cells from cultures of the control strain that were not induced, and induced with IPTG, respectively. The other details of this figure are the same as those described in Figure 17.

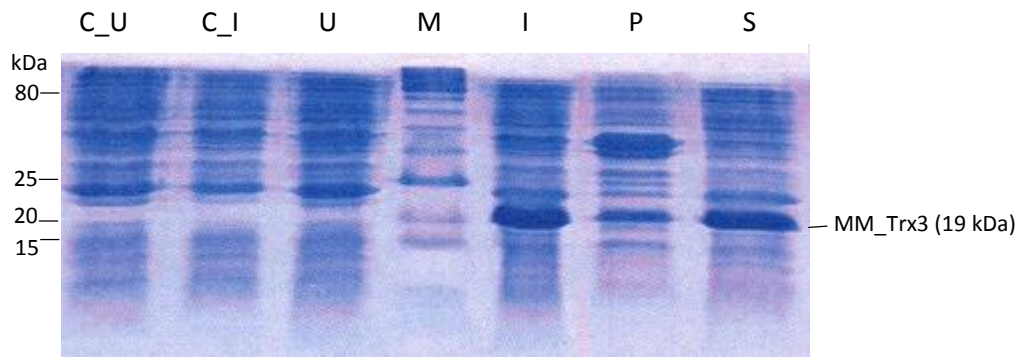


Figure 21. Expression of *M. mazei* MM_Trx3 (MM_2079) and its solubility in *E. coli*. SDS-PAGE analysis of cell extracts of *E. coli* strains: BL21(DE3)(pRIL)(pTev5), vector control and BL21(DE3)(pRIL)(pUL222), a strain expressing recombinant MM_Trx3. Details of this figure are the same as those described in Figure 17.

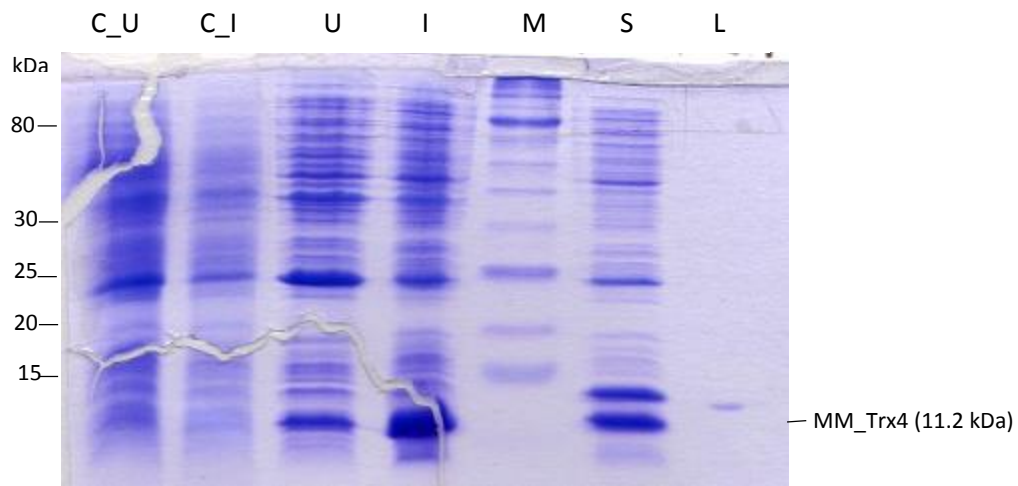


Figure 22. Expression of *M. mazei* MM_Trx4 (MM_2249) and its solubility in *E. coli*. SDS-PAGE analysis of cell extracts of *E. coli* strains: BL21(DE3)(pRIL)(pTev5), vector control and BL21(DE3)(pRIL)(pUL223), a strain expressing recombinant MM_Trx4. Details of this figure are the same as those described in Figure 17.

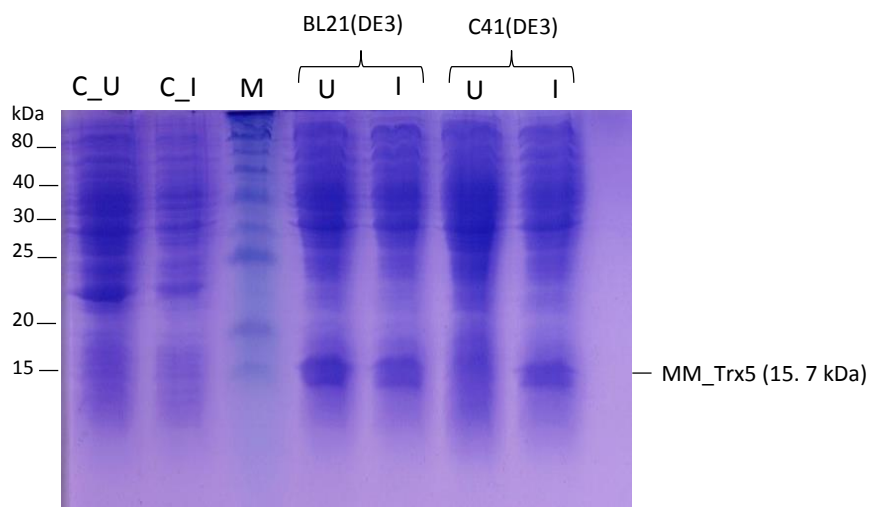


Figure 23. Expression of *M. mazei* MM_Trx5 (MM_2354) in *E. coli* strain BL21(DE3) and C41(DE3). SDS-PAGE analysis of cell extracts of *E. coli* strains with an expression vector carrying codon optimized *mm_2354*. The labels to the left of gel show the molecular mass values of the standards or markers in kDa and one on the right gives the location and molecular mass of MM_Trx5. C_U and C_I, cell extracts of control strain not induced and induced with IPTG. U and I, cell extracts of strains BL21(DE3)(pUL225) and C41(DE3)(pUL225), expressing recombinant MM_Trx5 and not induced and induced with IPTG, respectively.

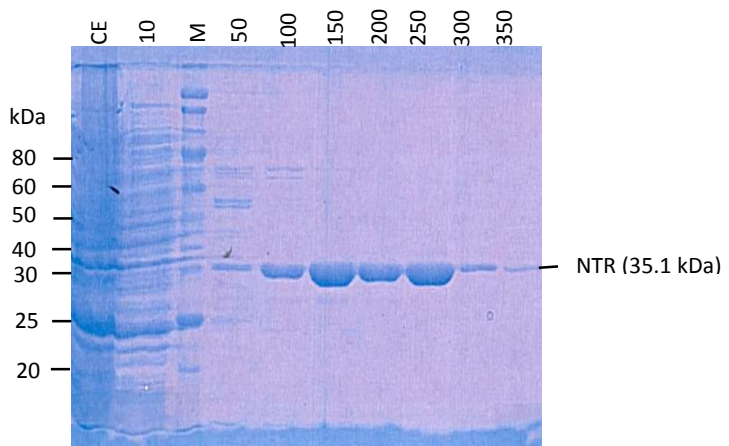


Figure 24. Purification of recombinant *M. mazei* NTR (MM_2353) via Ni^{2+} -affinity chromatography. Cell extracts and column fractions were analyzed via SDS-PAGE. The numbers above the gel are the concentrations of imidazole (10 mM to 350 mM) in elution buffers that eluted the respective fractions. Numbers to the left of the gel indicate the molecular mass values of the standards in kDa, and the label on the right shows the location and the molecular mass of the MM_NTR polypeptide. CE, cell extract. M, Molecular mass standards.

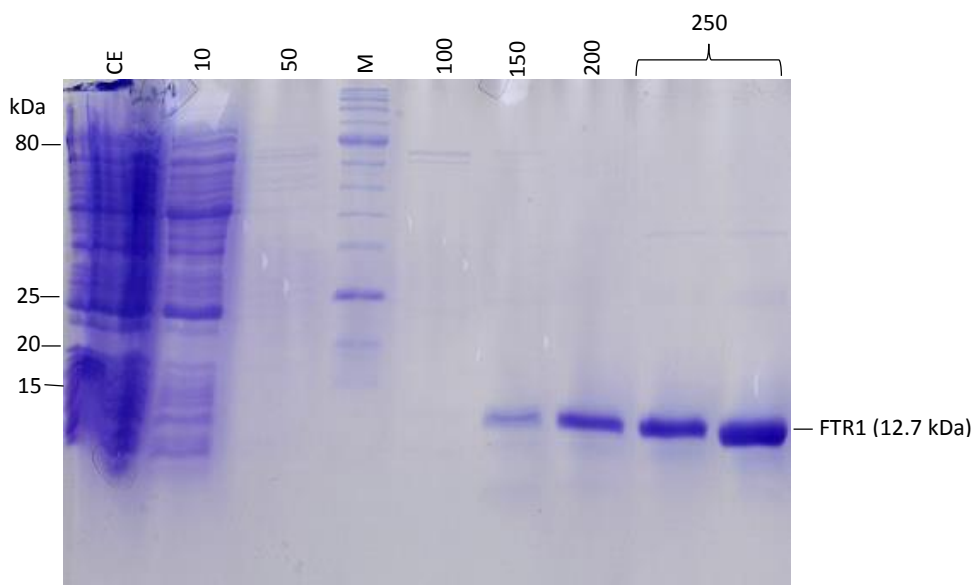


Figure 25. Purification of recombinant *M. mazei* FTR1 via Ni^{2+} -affinity chromatography. Cell extracts and column fractions were analyzed via SDS-PAGE. Details of this figure are the same as those described in Figure 24.

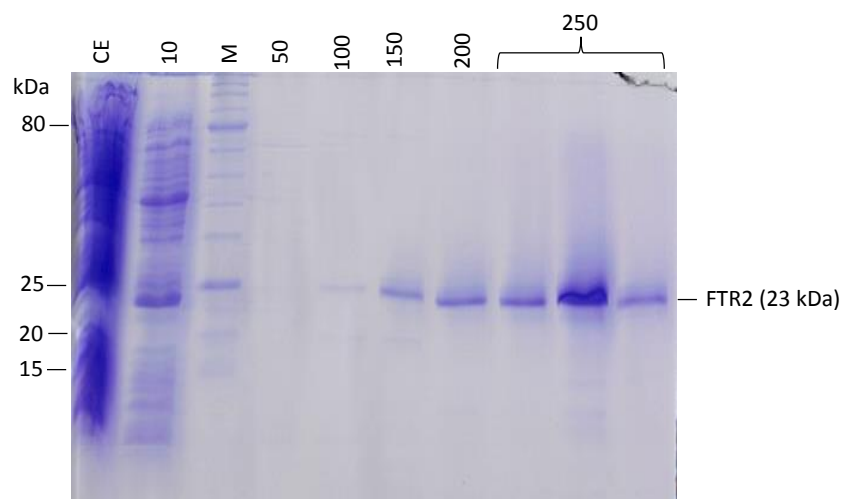


Figure 26. Purification of recombinant *M. mazei* FTR2 via Ni^{2+} -affinity chromatography. Cell extracts and column fractions were analyzed via SDS-PAGE. Details of this figure are the same as those described in Figure 24.

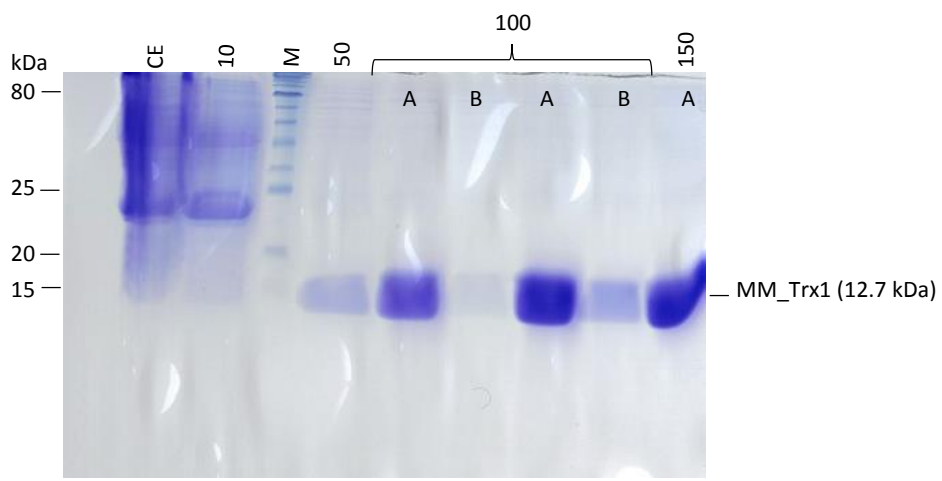


Figure 27. Purification of recombinant *M. mazei* MM_Trx1 (MM_0436) via Ni^{2+} -affinity chromatography. Cell extracts and column fractions were analyzed via SDS-PAGE. Details of this figure are the same as those described in Figure 24.

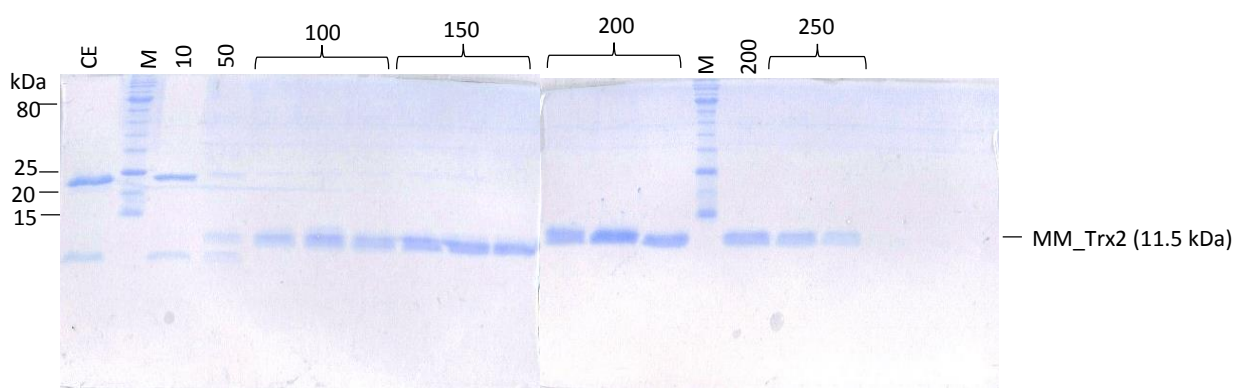


Figure 28. Purification of recombinant *M. mazei* MM_Trx2 (MM_0737) via Ni^{2+} -affinity chromatography. Cell extracts and column fractions were analyzed via SDS-PAGE. Details of this figure are the same as those described in Figure 24.

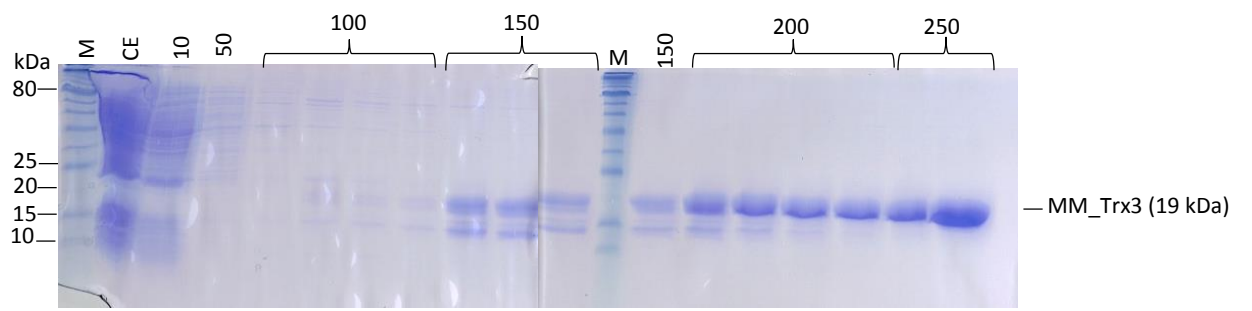


Figure 29. Purification of recombinant *M. mazei* MM_Trx3 (MM_2079) via Ni^{2+} -affinity chromatography. Cell extracts and column fractions were analyzed via SDS-PAGE. Details of this figure are the same as those described in Figure 24.

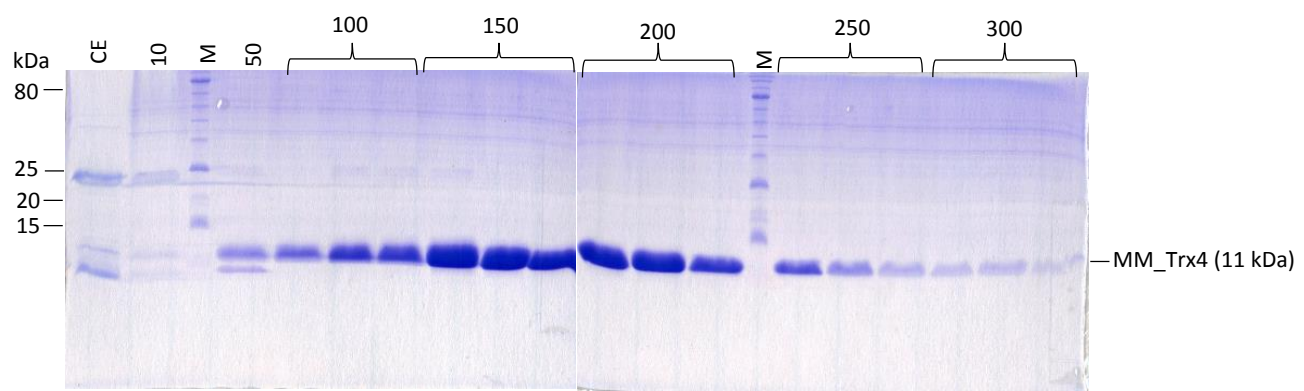


Figure 30. Purification of recombinant *M. mazei* MM_Trx4 (MM_2249) via Ni^{2+} -affinity chromatography. Cell extracts and column fractions were analyzed via SDS-PAGE. Details of this figure are the same as those described in Figure 24.

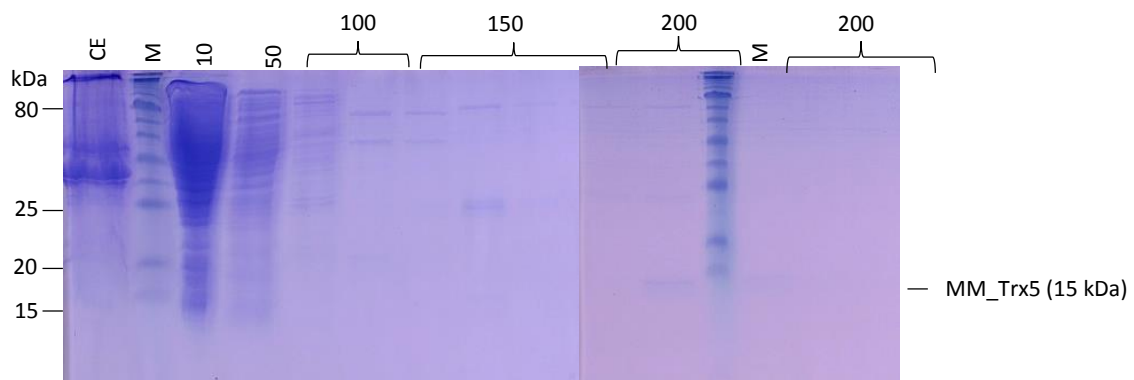


Figure 31. Purification of recombinant *M. mazei* MM_Trx5 (MM_2354) via Ni²⁺-affinity chromatography. Cell extracts and column fractions were analyzed via SDS-PAGE. Details of this figure are the same as those described in Figure 24.

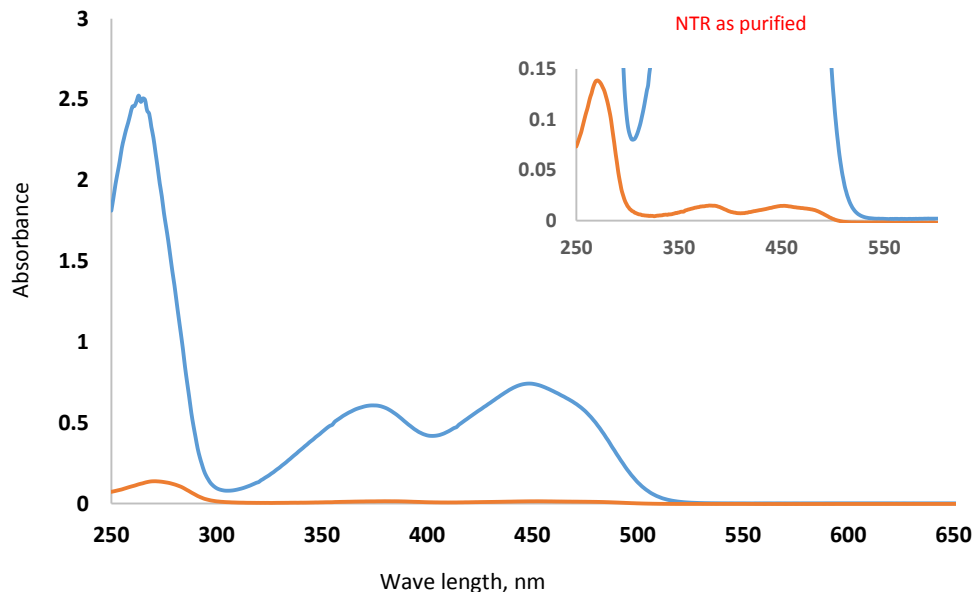


Figure 32. UV visible spectra of *M. mazei* NTR (MM_2353) as purified and after reconstitution with FAD. The spectra for NTR before and after reconstitution with FAD (final concentration in the reconstitution solution, 1 mM), are shown in red and blue, respectively. The protein concentration: as purified, 1 μ M; after reconstitution with FAD, 0.68 μ M. The inset is an expanded form of the spectrum of NTR before reconstitution. Both spectra show peaks at 375 nm and 450 nm, typical of flavin. Values of A_{450} : as purified, 0.0145; after reconstitution, 0.7418. Values of $A_{450}/\mu\text{M}$: as purified, 0.0145; after reconstitution, 1.09.

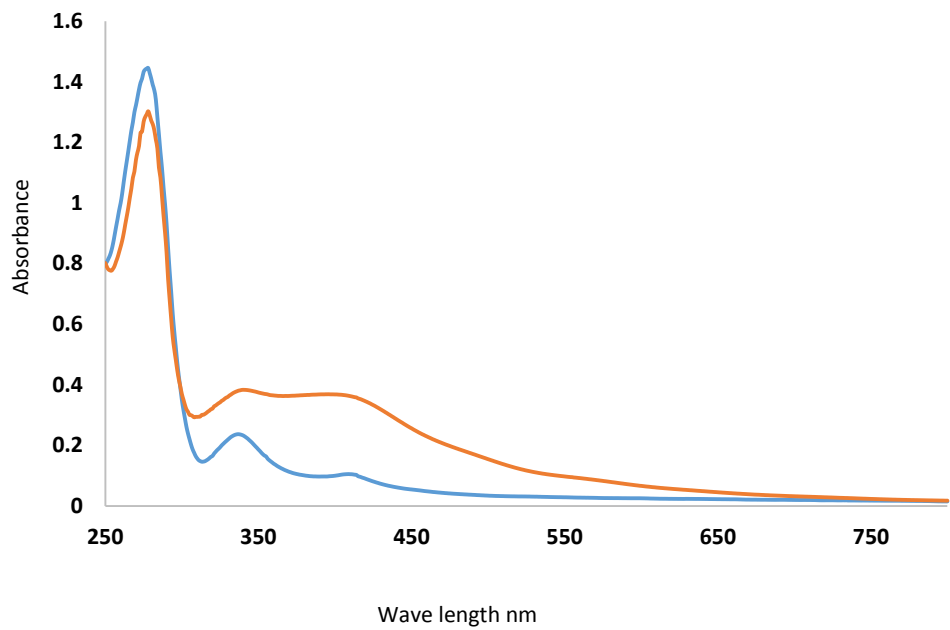


Figure 33. UV visible spectroscopy of *M. mazei* FTR1 (MM_0057) and FTR2 (MM_3270). The spectrum of FTR 1 (blue) and FTR 2 (red) show peaks at 340 nm and 410 nm, and 345 nm and 415 nm, respectively, which are typical of a [4Fe-4S] cluster [69]. The protein concentrations were 3.65 μ M for FTR1 and 3.98 μ M for FTR2.

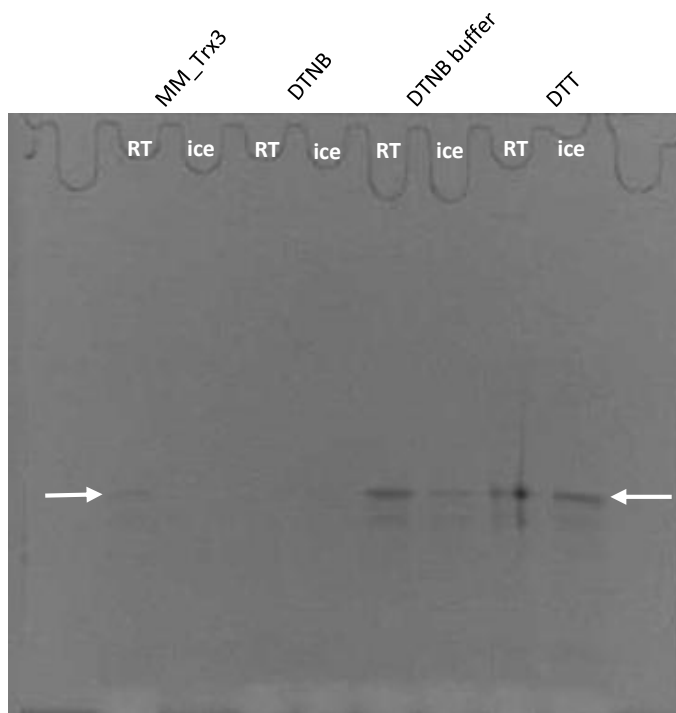


Figure 34. Oxidation and reduction of *M. mazei* MM_Trx3 (MM_2079). The SDS-PAGE gel of Trx3 treated with mBBr, a fluorescent probe viewed under 360 nm UV light. Lane MM_Trx3, Trx as purified and treated with mBBr; lane DTNB, Trx after oxidation with DTNB and labelled with mBBr; lane DTNB buffer, Trx in DTNB buffer (control) and labelled with mBBr; lane DTT, DTNB oxidized Trx reduced back with DTT and labelled with mBBr. Incubation temperatures (room temperature ~ 22°C, RT or on ice) is shown on top of the loading wells. The white arrows point to the location of the Trx band.

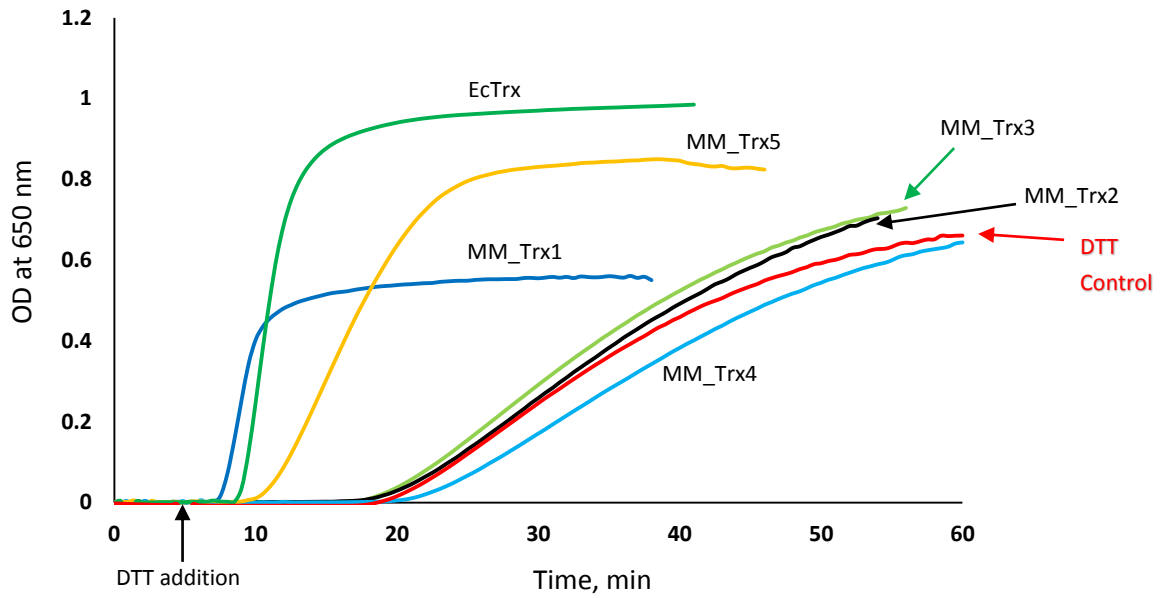


Figure 35. Insulin reduction activity of *Methanoscarcina mazei* Trxs and *Escherichia coli* Trx (EcTrx) with DTT as the electron donor. The reactions were performed at 37°C. After 5 min of initial observation, DTT was added to the Trx solution to a final concentration of 1 mM to start the reaction and the progress of the reaction was followed spectrophotometrically at 650 nm. The DTT control reaction was performed without Trx. OD, optical density.

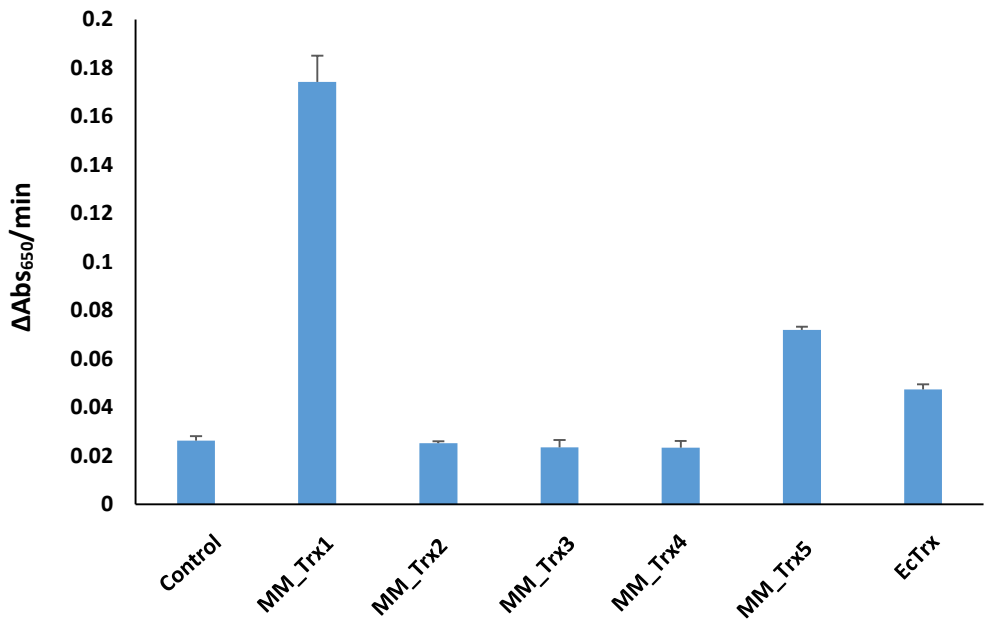


Figure 36. Insulin reduction activity for the Trxs of *Methanosaerina mazei* and *Escherichia coli* Trx (EcTrx). The data shown represents the rate (slope) values derived from progress curves similar to those shown in figure 35.

*Pairing of *M. mazei* TrxRs with its cognate Trxs*

*DTNB assay to pair *M. mazei* NTR (MM_NTR) with its cognate Trx*

In a control reaction, *E. coli* Trx successfully reduced DTNB in the presence of MM_NTR at an average rate of 0.028 min^{-1} . The electron flow followed the following scheme: $\text{NADPH} \rightarrow \text{MM_NTR} \rightarrow \text{EcTrx} \rightarrow \text{DTNB}$. In a similar reaction ($\text{NADPH} \rightarrow \text{MM_NTR} \rightarrow \text{MM_Trx} \rightarrow \text{DTNB}$) MM_Trx3 and MM_Trx5 reduced DTNB with an average rate of 0.17 min^{-1} and 0.03 min^{-1} respectively (Figure 37-38), while MM_Trx1 and MM_Trx4 did not reduce DTNB.

In assays conducted using *E. coli* thioredoxin reductase (EcNTR) as the enzyme, *E. coli* Trx and MM_Trx1 reduced DTNB with an average rate of 0.28 min^{-1} and 0.03 min^{-1} respectively, while all other *M. mazei* Trxs did not accept electrons from EcNTR to reduce DTNB (Figure 39). The electron flow scheme was $\text{NADPH} \rightarrow \text{Ec_NTR} \rightarrow \text{MM_Trx} \rightarrow \text{DTNB}$.

*Pairing of *M. mazei* FTR1 and 2 with its cognate Trx*

For pairing the FTRs with their cognate Trx, assays using different electron donors were tried and the following results were obtained.

Dithionite as electron donor for insulin reduction

When dithionite was used as the primary electron donor to reduce insulin, either in the presence of FTR1 or FTR2 as the electron transfer enzyme, the MM_Trx1, MM_Trx2, MM_Trx3 and MM_Trx4, did not reduce insulin. The electron flow scheme was dithionite $\rightarrow \text{MM_FTR} \rightarrow \text{MM_Trx} \rightarrow \text{insulin}$.

Clostridial ferredoxin as the electron donor for insulin reduction

Clostridial ferredoxin was reduced with hydrogen gas in the presence of *Clostridium pasteurianum* hydrogenase. Using this reduced ferredoxin as the electron donor for FTR1 the insulin reduction activities

of MM_Trx1, MM_Trx2, MM_Trx3, and MM_Trx4, were tested. The results were negative. The expected electron flow was $H_2 \rightarrow$ hydrogenase \rightarrow ferredoxin \rightarrow MM_FTR \rightarrow MM_Trx \rightarrow Insulin.

NADPH as the electron donor for the rubredoxin domain in FTR2 for the reduction of DTNB

Spinach FNR was used to catalyze the reduction of the rubredoxin domain of FTR2 with NADPH as the electron donor. None of the five MM_Trxs reduced DTNB in this assay. Expected electron flow route was NADPH \rightarrow FNR \rightarrow FTR2 \rightarrow MM_Trx \rightarrow DTNB.

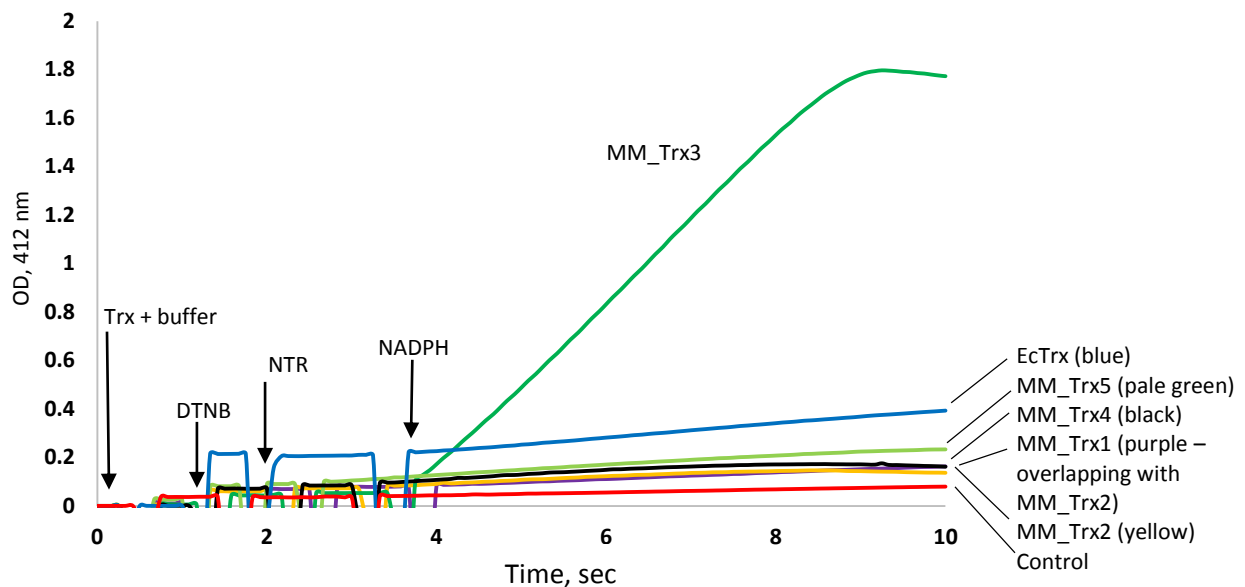


Figure 37. DTNB reduction activity of *Methanosaeca mazae* Trxs and *Escherichia coli* Trx with *M. mazae* NTR as the transfer enzyme. NADPH was the electron donor. MM_Trx3 was the only Trx that showed significant DTNB reduction activity in this assay; average rate was 0.3378 min^{-1} . The control assay was done without any Trx. The assay scheme: Trx + DTNB + NTR + NADPH → spectrophotometric observation at 412 nm. OD, optical density.

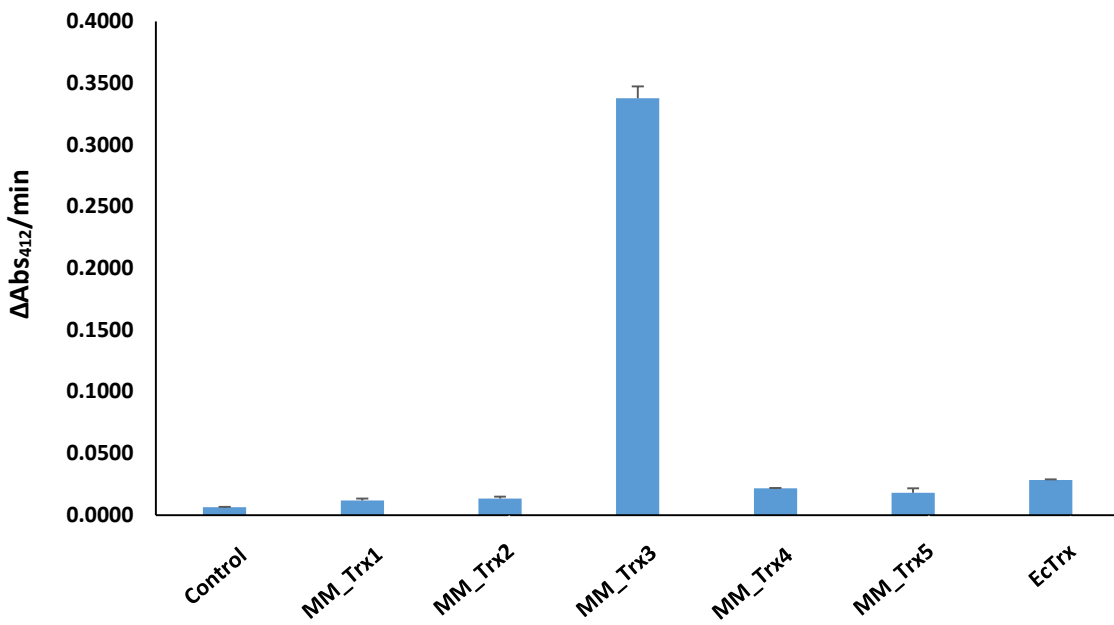


Figure 38. DTNB reduction activities of Trxs from *Methanosaicina mazei* (MM_Trx1 – 5) and *Escherichia coli* (EcTrx) with *M. mazei* NTR as the electron transfer enzyme. The data shown represents the rate (slope) values derived from progress curves similar to those shown in Figure 37. The control reaction was performed without the addition of a Trx. MM_Trx3 was the only Trx to reduce DTNB significantly.

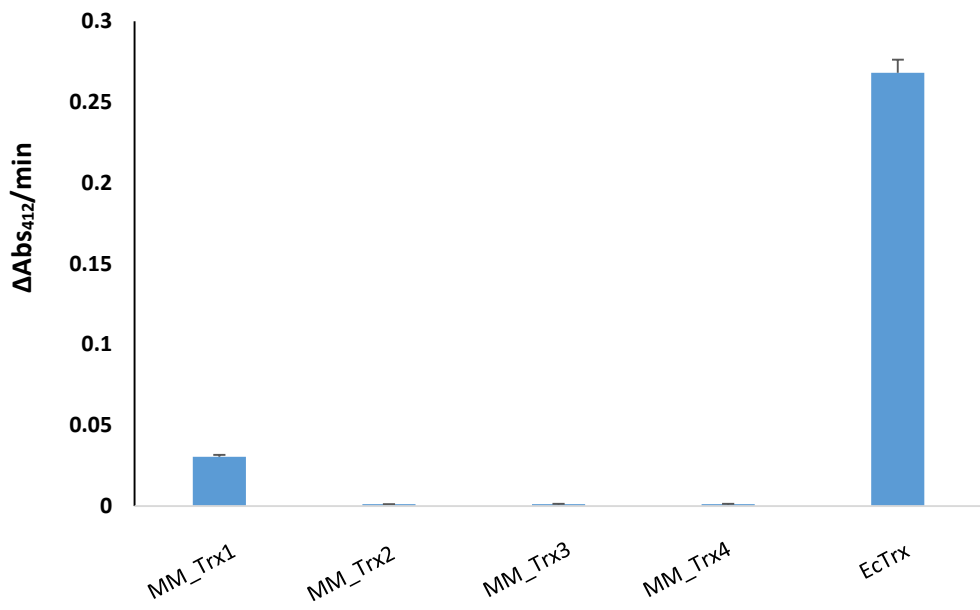


Figure 39. DTNB reduction activities of *Escherichia coli* Trx (EcTrx) and *Methanosaerica mazei* Trxs with *E. coli* NTR as the electron transfer enzyme. The control reaction was performed without the addition of a Trx. MM_Trx1 was the only *M. mazei* Trx to accept electrons from *E. coli* NTR and reduce DTNB.

Chapter 4: DISCUSSION

Thioredoxin and thioredoxin reductase homologs in *Methanosarcina mazei*

The study conducted from our laboratory indicates that methanogenic archaea carry 2 to 8 Trx homologs, except *Methanopyrus kandleri* which seems to lack such a protein [42]. The deeply rooted methanogens which have smaller genomes and use mainly H₂ and CO₂ as methanogenic substrates, have about 2 to 4 Trx homologs, while the late evolving methanogens that have larger genomes and use a variety of substrates, have anywhere between 2 to 8 Trx homologs [42]. *Methanosarcina mazei* possesses five thioredoxin homologs, ranging in size from 8 kDa to 15 kDa, and three thioredoxin reductase homologs, whereas the deeply rooted methanogenic archaeon *Methanocaldococcus jannaschii* has only two thioredoxins and one thioredoxin reductase homolog (Figure 3) [42]. A recently published study on the thioredoxin system of *Methanosarcina acetivorans* indicates *M. mazei* to have seven putative thioredoxin homologs. In addition to the five Trxs reported in my study, the genes *mm_0991* and *mm_2240* have been also implicated as putative thioredoxins [71]. NCBI has annotated *mm_0991* as a thiol-disulfide isomerase, and *mm_2240* as a hypothetical protein, and both of these proteins are larger (18kDa and 21kDa, respectively) than typical Trxs, and were therefore not included in my study. The amino acid sequences of MM_0991 and MM_2240 show an active site motif of CXXC, and the proteins may have the thioredoxin fold. The disulfide reducing properties of these two proteins are yet to be verified.

From a comparison of the amino acid sequences of the five *M. mazei* Trxs analyzed in this study, with the Trxs of *E. coli*, *Clostridium* sp., and other *Methanosarcina* species, I found MM_Trx1 to be more of a bacterial origin. The active site motif of CGPC in MM_Trx1 is similar to that of *E. coli* Trx, and the protein exhibits a robust insulin reduction ability and accepts electrons from *E. coli* NTR but not from *M. mazei* NTR. All these properties indicates its bacterial origin. These results further support the hypothesis

of lateral gene transfer between bacteria and archaea [15]. It is not clear at this stage which of the Trx reductases reduces this Trx *in vivo*. The amino acid sequence comparison also indicated that the remaining Trxs and the TrxRs are of archaeal ancestry.

Characteristics of *M. mazei* thioredoxins

Each of the *M. mazei* Trxs were over-expressed in soluble forms in *E. coli*, except for MM_Trx5 which was expressed in very low amount (Figure 16-23). The over-expressed recombinant Trxs were purified to homogeneity using the Ni²⁺ affinity chromatography (Figure 24-31). Poor expression of MM_Trx5 in *E. coli* was likely due to the toxicity of this protein; survival of the host was affected after induction (data not shown). The other explanation is that recombinant MM_Trx5 did not fold well and was degraded by the host. We considered the possibility that MM_Trx5 (MM_2354) and MM_NTR (MM_2353) associate in the cell, promoting folding and stabilizing the former. The genes for these proteins form an operon. To leverage this possibility, co-expression of MM_Trx5 and the NTR in *E. coli* BL21(DE3)(pRIL) was attempted. This system resulted in the over-expression of the NTR and very low expression of MM_Trx5. Expression trials in *E. coli* and subsequent Ni²⁺ affinity purification, with a codon optimized gene produced barely enough MM_Trx5 protein for assays. These results suggest that MM_Trx5 is toxic to its un-natural host, and/or perhaps was destroyed by the host proteases even when co-expressed with the NTR.

When performing the DTNB assay for pairing NTR with its cognate Trx, the purified Trxs were found in various oxidation states. MM_Trx1, and MM_Trx5 were always in reduced states, where as MM_Trx2, MM_Trx3, and MM_Trx4 were sometimes found in oxidized states. As a result MM_Trx1 and MM_Trx5 reduced DTNB readily before the addition of NTR and the electron donor NADPH, and with MM_Trx2, MM_Trx3 and MM_Trx4 this reaction occurred in most but not all cases. It is possible that the observed variability in the oxidation states of the as purified preparations of MM_Trx2, MM_Trx3, and

MM_Trx4 was due to the fact that their active site cysteines were more exposed to the solvent and consequently were prone to oxidation. It could also be due to the differences in mid-point redox potentials of the Trxs.

Insulin reduction assay is the most common disulfide reducing assay used for characterizing a thioredoxin, and we used the same in this study. MM_Trx1 and MM_Trx5 exhibited high rates of insulin disulfide reduction and short lag times, but MM_Trx2, MM_Trx3, and MM_Trx4 were unable to reduce insulin in these kinetic assays (Figure 35-36). Not all Trxs can reduce insulin very effectively, as is the case with *Methanocaldococcus jannaschii* Trx2 which had 80-fold lower insulin reduction activity compared to the other Trx (Trx1) of the same organism [42]. The rates and the lag time in insulin reduction assay have been traditionally used to characterize the disulfide reducing activities of Trxs [49], but these two factors do not always correlate with each other. There are three disulfide bonds in insulin and different Trxs could reduce these bonds differently depending on the redox potentials of their catalytic Cys pairs. The lag time on the other hand is linked to the accessibility of the disulfide bonds in insulin to a Trx. Hence, the insulin reduction assay involves a set of complex processes, which render it less effective in a quantitative and precise measurement. Even though MM_Trx3 was unable to reduce insulin, it reduced DTNB at a very high rate, when electrons were provided from NADPH via NTR (Figure 37-38). MM_Trx2, and MM_Trx4 could not reduce insulin because their active site cysteines were not readily reduced by DTT. This explanation was inferred from the fact that when oxidized forms of these Trxs were treated with DTT and mBBr, the proteins did not exhibit the characteristic UV-fluorescence in a SDS_PAGE gel. For MM_Trx3, the reason for the lack of insulin reduction activity remains unclear, as DTT was able to reduce this protein. Perhaps a different method for assaying disulfide reduction, such as one via the activation of methionine sulfoxide or the ribonucleotide reductase should be used for examining this Trx.

The problems of expressing the *M. mazei* Trxs in *E. coli* at high levels, the production of Trxs at various oxidation states, the inability to reduce insulin, all could perhaps be solved by expressing these

archaeal proteins in a *Methanosarcina* sp., and purifying these anaerobically. These approaches may also result in better protein-protein interactions. Modeling of the Trx structures would help to shed light on the interaction of the active sites of these proteins with insulin or other targets.

Thioredoxin – thioredoxin reductase systems of *Methanosarcina mazei*

Very few of the thioredoxin – thioredoxin reductase systems of archaea have been characterized. Previous work in this area has been with the archaea *Sulfolobus solfataricus*, *Pyrococcus horikoshii*, *Aeropyrum pernix* and *Methanocaldococcus jannaschii* [42, 70, 72, 73]. In case of *Thermoplasma acidophilum*, and *M. jannaschii*, a TrxR and Trx form a thioredoxin system, but the respective electron donor is unknown [42, 74]. The Trx1 (MJ0307) of *M. jannaschii* has been found to be involved in the activation of deactivated methanogenesis and cell biosynthesis enzymes [42]. A recent study on *Methanosarcina acetivorans* describes an NADPH dependent NTR – Trx system, that recognizes one of the eight Trxs of this organism [71]. This finding is similar to our observation that one of the Trxs (MM_Trx3) of *M. mazei* was recognized by the NADPH dependent TrxR of this organism (Figure 37-38).

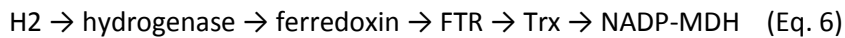
The FTR – Trx system, which is dependent on reduced ferredoxin for electron delivery, is very well studied in plants, especially in spinach, green algae, and oxygenic prokaryotes such as cyanobacteria [55], as well as in a *Clostridium* species [69]. Several FTR – Trx systems target enzymes involved in starch metabolism, lipid and amino acid biosynthesis, to name a few [57, 60]. In plant FTR – Trx system, low potential electrons generated by light at the photosystem of chloroplast are transferred to ferredoxin, and then the electrons from reduced ferredoxin are transferred to a thioredoxin via the Fe-S cluster of the FTR [75]. In non-photosynthetic bacteria, ferredoxin is reduced by NADPH or H₂ by the action of ferredoxin NADP reductase (FNR) or hydrogenase [69].

The FTR – Trx systems of the archaea are yet to be fully characterized. The assays used in my study did not allow a detailed characterization of the FTR – Trx systems of *M. mazei*. *M. mazei* has two FTRs,

one NTR, 5 Trxs and eighteen ferredoxin homologs, which makes it difficult to characterize the FTR-Trx systems of this archaea. Various assays have been used to study the plant FTR – Trx system [59, 69]. The fructose 1,6-bisphosphatase (FBPase) assay is one of the examples which involves the reduction of ferredoxin with dithionite. Reduced ferredoxin then reduces Trx via FTR, which finally reduces and activates FBPase [59]. The active FBPase activity is coupled to phosphoglucose isomerase and glucose-6-phosphate dehydrogenase leading to the reduction of NADP⁺ which is observed spectrophotometrically as an increase in absorbance at 340nm [59]. Schematic representation of electron flow is shown below.



The NADP-malate dehydrogenase (NADP-MADH) assay has been used to study the FTR – Trx system in *Clostridium pasteurianum* [69]. This assay is conducted anaerobically in the presence of H₂ gas, and the reduction of ferredoxin is catalyzed by a hydrogenase [69]. Trx is reduced by the reduced ferredoxin via FTR. The activation of NADP-malate dehydrogenase by reduced Trx results in the oxidation of NADPH by oxaloacetate which is observed at 340nm [69]. The electron flow for this reaction is as follows:



Perhaps one such assay might help to characterize the FTR – Trx system in *M. mazei* and one needs to find a suitable target enzyme for activation (Eqs. 5 & 6).

In *M. mazei* the gene for FTR2 apparently forms an operon with an upstream putative glutaredoxin (Grx) gene. Most organisms that have a Grx, NADPH is the electron donor for glutathione reductase (GR) that reduces glutathione, which subsequently reduces Grx. In case of the cyanobacteria *Synechocystis*, the Grx is reduced by NTR and not by a GR, and forms a unique NTR – Grx system [76]. Methanogens lack glutathione [77, 78]. Perhaps the presence of the putative *grx* – *ftr2* operon in *Methanosarcina* species suggests the existance of a unique FTR – Grx system in these organisms. A proposed utility of a FTR2 – Grx or FTR2 – Grx – Trx system in *M. mazei* is shown in Figure 40.

FTR2 of *M. mazei* also has a C-terminal rubredoxin (Rd) domain, the only Rd in this organism. The superoxide reductase (SOR) of *M. mazei* requires rubredoxin as electron donor to detoxify superoxide and form hydrogen peroxide [33]. I believe FTR2 to be the electron donor for SOR. A proposed mechanism for the reduction of SOR is shown in Figure 40.

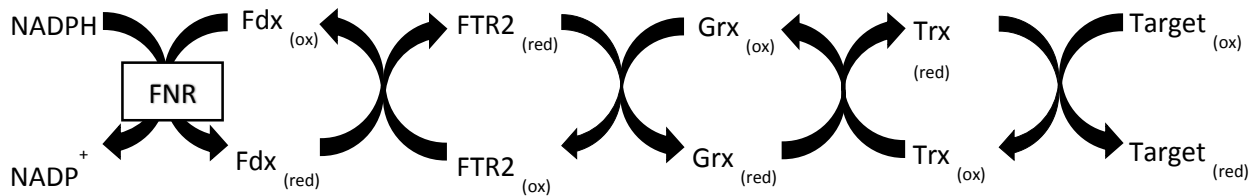
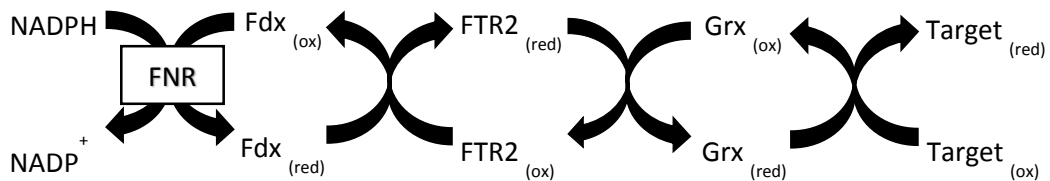
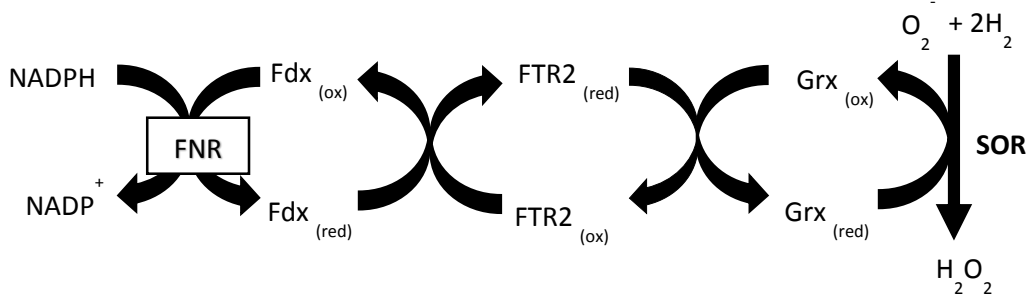
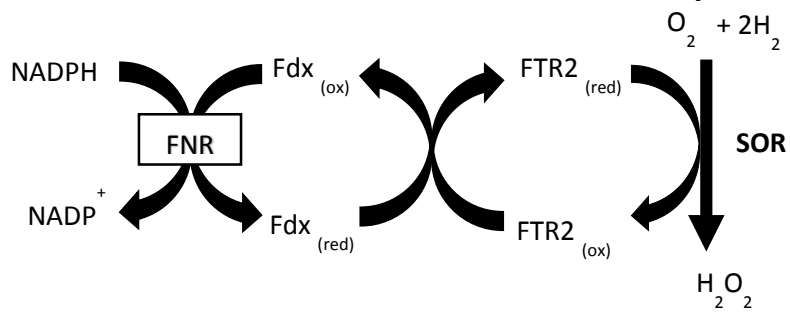


Figure 40. Proposed utilities of FTR2 – Trx/Grx systems in *Methanosarcina mazei*

CONCLUSION

In this study I have characterized the thioredoxin system of *M. mazei*. The findings of this study have been summarized in Table 2. Five thioredoxin homologs of the archaeon were successfully expressed and purified to homogeneity. A high rate of disulfide reduction activity was found in MM_Trx1 and in MM_Trx5 via insulin assay, and MM_Trx3 by DTNB reduction assay. I have shown that MM_Trx3 accepts electrons from NTR to form a complete NTR – Trx system in *M. mazei*. The FTR – Trx system has been extensively studied in plants, but is yet to be characterized in archaea. Here I have proposed several possible mechanisms for FTR2, one of which is to form a complete system with glutaredoxin (Grx) and Trx(s). I have also suggested the possibility that in *M. mazei* FTR2 reduces a SOR during oxidative stress, as it carries the sole rubredoxin of this organism in its C – terminal domain, which is necessary for the activity of SOR.

Characterizing the thioredoxin system of *M. mazei* has laid the foundation for an investigation of how the organism deals with oxidative stress and implement redox control of metabolism. It is possible for FTR2 and Grx to allow MM_Trx1 to reduce target proteins involved in combating oxidative stress and redox regulation. This study will help to fulfill the goal of finding the target proteins for each of the Trxs. The findings in this study also indicate a need for a better method of assaying for archaeal FTR – Trx systems.

Table 2. Characteristics of the thioredoxin system of *Methanosarcina mazei*.

Homolog designation	ORF number (MM_)	MW with 6His tag (g/mole)	pI with -out 6His tag	Trx active site motif	Operon with another gene	Insulin reduction activity	DTNB reduction activity		Closest relative in terms of % Identity & Similarity	Comments
							with electrons from MM_NTR	with electrons from Ec_NTR		
MM_Trx1	0436	12675.49	5.34	CGPC	No	Yes	No	Yes	<i>Clostridium</i>	CGPC motif similar to <i>E. coli</i> Trx
MM_Trx2	0737	8754.5	8.51	CAKC	No	No	No	No	<i>Methanocaldococcus jannaschii</i> Trx2	
MM_Trx3	2079	18707.78	5.36	CPYC	No	No	Yes	No	<i>Methanocaldococcus jannaschii</i> Trx1	CPYC motif typical for glutaredoxin
MM_Trx4	2249	11208.01	7.71	CPKC	No	No	No	No	<i>Methanocaldococcus jannaschii</i> Trx1	CPKC motif similar to the active site motif of MjTrx2
MM_Trx5	2354	15708.62	5.09	CTAC	Yes	Yes	No	No	<i>Methanocaldococcus jannaschii</i> Trx1	<i>mm_2354</i> (MM_Trx5) forms an operon with <i>mm_2353</i> (NTR)
NTR	2353	35080.02	5.51	CATC	Yes	—	—	—	<i>Methanosarcina</i>	Same as above
FTR 1	0057	12714.27	5.37	CPCX14CPCX12CHC	No	—	—	—	<i>Methanosarcina</i>	
FTR 2	3270	22971.91	4.93	CPCX14CPCX12CYC	Yes	—	—	—	<i>Methanosarcina</i>	In operon with a glutaredoxin gene <i>mm_3271</i>

, not applicable.

REFERENCES

1. Deppenmeier, U., et al., *Reduced coenzyme F420: heterodisulfide oxidoreductase, a proton-translocating redox system in methanogenic bacteria*. Proceedings of the National Academy of Sciences, 1990. **87**(23): p. 9449-9453.
2. Boone, D.R., W.B. Whitman, and P. Rouviere, *Microbiology, diversity and taxonomy of methanogens*. Methanogenesis: ecology, physiology, biochemistry and genetics. 1993, New York, NY: Chapman and Hall. 35-80.
3. Zinder, S.H., *Microbiology, physiology ecology of methanogens*. Methanogenesis: ecology, physiology, biochemistry and genetics. 1993, New York, NY: Chapman and Hall.
4. Wolfe, R.S., *1776-1996: Alessandro Volta's Combustible Air. 220 years after Volta's experiments, the microbial formation of methane approaches an understanding*. American Society for Microbiology, 1996. **62**(10): p. 529-534.
5. Franzmann, P.D., et al., *Methanogenium frigidum sp. nov., a Psychrophilic, H₂-Using Methanogen from Ace Lake, Antarctica*. International Journal of Systematic Bacteriology, 1997. **47**(4): p. 1068-1072.
6. Daniels, L., *Biological methanogenesis: physiological and practical aspects*. Trends in Biotechnology, 1984. **2**(4): p. 91-98.
7. Ferry, J.G., *Fermentation of acetate*. Methanogenesis: ecology, physiology, biochemistry, and genetics. 1993, New York, NY: Chapman and Hall.
8. Thauer, R.K., et al., *Methanogenic archaea: ecologically relevant differences in energy conservation*. Nature Reviews: Microbiology, 2008. **6**.
9. Alkanok, G., B. Demirel, and T.T. Onay, *Determination of biogas generation potential as a renewable energy source from supermarket wastes*. Waste Management, (0).
10. Ferry, J.G., *Enzymology of the fermentation of acetate to methane*. Biofactors, 1997. **6**(1): p. 25.
11. Rothman, D.H., et al., *Methanogenic burst in the end-Permian carbon cycle*. Proceedings of the National Academy of Sciences, 2014. **111**(15): p. 5462-5467.
12. De Vrieze, J., et al., *Methanosarcina: The rediscovered methanogen for heavy duty biomethanation*. Bioresource Technology, 2012. **112**(0): p. 1-9.
13. Fournier, G.P. and J.P. Gogarten, *Evolution of Acetoclastic Methanogenesis in Methanosarcina via Horizontal Gene Transfer from Cellulolytic Clostridia*. Journal of Bacteriology, 2008. **190**(3): p. 1124-1127.
14. Ingram-Smith, C., S.R. Martin, and K.S. Smith, *Acetate kinase: not just a bacterial enzyme*. Trends in Microbiology, 2006. **14**(6): p. 249-253.
15. Deppenmeier, U., et al., *The genome of Methanosarcina mazei: Evidence for lateral gene transfer between bacteria and archaea*. Journal of Molecular Microbiology Biotechnology, 2002. **4**(4).
16. Bult, C.J., et al., *Complete Genome Sequence of the Methanogenic Archaeon, Methanococcus jannaschii*. Science, 1996. **273**(5278): p. 1058-1073.
17. Sigler, K., et al., *Oxidative stress in microorganisms—I*. Folia Microbiologica, 1999. **44**(6): p. 587-624.
18. JA., I., *How oxygen damages microbes: oxygen tolerance and obligate anaerobiosis*. Adv Microb Physiol., 2002(46): p. 111-53.
19. Storz G, I.J., *Oxidative stress*. Curr Opin Microbiol., 1999 April **2**(2): p. 188-94.

20. Winterbourn, C.C., *Toxicity of iron and hydrogen peroxide: the Fenton reaction*. Toxicology Letters, 1995. **82–83**(0): p. 969-974.
21. Imlay, J.A., *Iron-sulphur clusters and the problem with oxygen*. Molecular Microbiology, 2006. **59**(4): p. 1073-1082.
22. Keyer, K. and J.A. Imlay, *Superoxide accelerates DNA damage by elevating free-iron levels*. Proceedings of the National Academy of Sciences, 1996. **93**(24): p. 13635-13640.
23. Cooke, M.S., et al., *Oxidative DNA damage: mechanisms, mutation, and disease*. FASEB J, 2003. **17**(10): p. 1195-214.
24. Kohen, R. and A. Nyska, *Invited Review: Oxidation of Biological Systems: Oxidative Stress Phenomena, Antioxidants, Redox Reactions, and Methods for Their Quantification*. Toxicologic Pathology, 2002. **30**(6): p. 620-650.
25. Cabisco E, T.J., Ros J., *Oxidative stress in bacteria and protein damage by reactive oxygen species*. Int Microbiol., 2000. **3**(1): p. 3-8.
26. Brioukhanov, A.L., A.I. Netrusov, and R.I.L. Eggen, *The catalase and superoxide dismutase genes are transcriptionally up-regulated upon oxidative stress in the strictly anaerobic archaeon Methanoscincus barkeri*. Microbiology, 2006. **152**(6): p. 1671-1677.
27. Jenney, F.E., et al., *Anaerobic Microbes: Oxygen Detoxification Without Superoxide Dismutase*. Science, 1999. **286**(5438): p. 306-309.
28. Cannio R, F.G., Morana A, Rossi M, Bartolucci S., *Oxygen: friend or foe? Archaeal superoxide dismutases in the protection of intra- and extracellular oxidative stress*. Front Biosci. , 2000. **1**(5): p. D768-79.
29. Zámocký, M., et al., *Molecular evolution of hydrogen peroxide degrading enzymes*. Archives of Biochemistry and Biophysics, 2012. **525**(2): p. 131-144.
30. Díaz, A., et al., *Thirty years of heme catalases structural biology*. Archives of Biochemistry and Biophysics, 2012. **525**(2): p. 102-110.
31. Brines, L.M. and J.A. Kovacs, *Understanding the Mechanism of Superoxide Reductase Promoted Reduction of Superoxide*. European Journal of Inorganic Chemistry, 2007. **2007**(1): p. 29-38.
32. Santos-Silva, T., et al., *The first crystal structure of class III superoxide reductase from Treponema pallidum*. JBIC Journal of Biological Inorganic Chemistry, 2006. **11**(5): p. 548-558.
33. Krätzer, C., et al., *Methanoferrodoxin represents a new class of superoxide reductase containing an iron–sulfur cluster*. FEBS Journal, 2011. **278**(3): p. 442-451.
34. Lu, J. and A. Holmgren, *The thioredoxin antioxidant system*. Free Radical Biology and Medicine, 2014. **66**(0): p. 75-87.
35. Holmgren, A., *Thioredoxin*. Annual Review: Biochemistry, 1985. **54**.
36. Collet JF, M.J., *Structure, function, and mechanism of thioredoxin proteins*. Antioxid Redox Signal., 2010. **13**(8): p. 1205-16.
37. Rocha, E.R., A.O. Tzianabos, and C.J. Smith, *Thioredoxin Reductase Is Essential for Thiol/Disulfide Redox Control and Oxidative Stress Survival of the Anaerobe Bacteroides fragilis*. Journal of Bacteriology, 2007. **189**(22): p. 8015-8023.
38. Serata, M., et al., *Roles of thioredoxin and thioredoxin reductase in the resistance to oxidative stress in Lactobacillus casei*. Microbiology, 2012. **158**(Pt 4): p. 953-962.
39. Cha, M.-K., H.-K. Kim, and I.-H. Kim, *Thioredoxin-linked "Thiol Peroxidase" from Periplasmic Space of Escherichia coli*. Journal of Biological Chemistry, 1995. **270**(48): p. 28635-28641.
40. Zhang, X.-H. and H. Weissbach, *Origin and evolution of the protein-repairing enzymes methionine sulphoxide reductases*. Biological Reviews, 2008. **83**(3): p. 249-257.
41. Tsang, M.L. and J.A. Schiff, *Assimilatory sulfate reduction in an Escherichia coli mutant lacking thioredoxin activity*. Journal of Bacteriology, 1978. **134**(1): p. 131-138.

42. Susanti, D., et al., *Thioredoxin targets fundamental processes in a methane producing archaeon, Methanocaldococcus jannaschii*. PNAS, 2013.
43. Åslund, F. and J. Beckwith, *The Thioredoxin Superfamily: Redundancy, Specificity, and Gray-Area Genomics*. Journal of Bacteriology, 1999. **181**(5): p. 1375-1379.
44. Porqué, P.G., A. Baldesten, and P. Reichard, *The Involvement of the Thioredoxin System in the Reduction of Methionine Sulfoxide and Sulfate*. Journal of Biological Chemistry, 1970. **245**(9): p. 2371-2374.
45. A., H., *Hydrogen donor system for Escherichia coli ribonucleoside-diphosphate reductase dependent upon glutathione*. Proc Natl Acad Sci U S A, 1976. **3**(7): p. 2275-9.
46. Holmgren, A., I. Ohlsson, and M.L. Grankvist, *Thioredoxin from Escherichia coli. Radioimmunological and enzymatic determinations in wild type cells and mutants defective in phage T7 DNA replication*. Journal of Biological Chemistry, 1978. **253**(2): p. 430-436.
47. Holmgren, A., *Bovine thioredoxin system. Purification of thioredoxin reductase from calf liver and thymus and studies of its function in disulfide reduction*. Journal of Biological Chemistry, 1977. **252**(13): p. 4600-4606.
48. Arnér ES, H.A., *Measurement of thioredoxin and thioredoxin reductase*. Curr Protoc Toxicol, 2001.
49. Holmgren, A., *Thioredoxin catalyzes the reduction of insulin disulfides by dithiothreitol and dihydrolipoamide*. Journal of Biological Chemistry, 1979. **254**(19): p. 9627-9632.
50. Williams, C.H., et al., *Thioredoxin reductase*. European Journal of Biochemistry, 2000. **267**(20): p. 6110-6117.
51. Moore, E.C., P. Reichard, and L. Thelander, *Enzymatic Synthesis of Deoxyribonucleotides: V. PURIFICATION AND PROPERTIES OF THIOREDOXIN REDUCTASE FROM ESCHERICHIA COLI B*. Journal of Biological Chemistry, 1964. **239**(10): p. 3445-3452.
52. Hirt, R.P., et al., *The diversity and evolution of thioredoxin reductase: new perspectives*. Trends in Parasitology, 2002. **18**(7): p. 302-308.
53. Mustacich D, P.G., *Thioredoxin reductase*. Biochem J., 2000. **15**(346): p. 1:1-8.
54. Balsara, M., et al., *Ferredoxin:thioredoxin reductase (FTR) links the regulation of oxygenic photosynthesis to deeply rooted bacteria*. Planta, 2013. **237**(2): p. 619-635.
55. Buchanan B. B, et al., *The ferredoxin/thioredoxin system: from discovery to molecular structures and beyond*. Photosynth Res, 2002. **73**(1-3): p. 215-22.
56. Dai, S., et al., *Redox Signaling in Chloroplasts: Cleavage of Disulfides by an Iron-Sulfur Cluster*. Science, 2000. **287**(5453): p. 655-658.
57. Balmer, Y., et al., *A complete ferredoxin/thioredoxin system regulates fundamental processes in amyloplasts*. Proceedings of the National Academy of Sciences of the United States of America, 2006. **103**(8): p. 2988-2993.
58. Xu, X., et al., *Ternary Protein Complex of Ferredoxin, Ferredoxin:Thioredoxin Reductase, and Thioredoxin Studied by Paramagnetic NMR Spectroscopy*. Journal of the American Chemical Society, 2009. **131**(48): p. 17576-17582.
59. Schürmann, P., *Ferredoxin-dependent thioredoxin reductase: a unique iron-sulfur protein*. Methods Enzymol., 2002. **347**: p. 403-11.
60. Schürmann P and B.B. B., *The ferredoxin/thioredoxin system of oxygenic photosynthesis*. Antioxid Redox Signal., 2008. **10**(7): p. 1235-74.
61. Fetzer, S., F. Bak, and R. Conrad, *Sensitivity of methanogenic bacteria from paddy soil to oxygen and desiccation*. FEMS Microbiology Ecology, 1993. **12**(2): p. 107-115.
62. Rocco, C.J., et al., *Construction and use of new cloning vectors for the rapid isolation of recombinant proteins from Escherichia coli*. Plasmid, 2008. **59**(3): p. 231-237.

63. Case, C.L., J.R. Rodriguez, and B. Mukhopadhyay, *Characterization of an NADH oxidase of the flavin-dependent disulfide reductase family from Methanocaldococcus jannaschii*. Microbiology, 2009. **155**(1): p. 69-79.
64. Bradford, M.M., *A rapid and sensitive method for the quantification of microgram quantities of protein utilizing the principle of protein-dye binding*. Analytical Biochemistry, 1976(72): p. 248-254.
65. Mukhopadhyay, B., et al., *Cloning, Sequencing, and Transcriptional Analysis of the Coenzyme F420-dependent Methylene-5,6,7,8-tetrahydromethanopterin Dehydrogenase Gene from Methanobacterium thermoautotrophicum Strain Marburg and Functional Expression in Escherichia coli*. Journal of Biological Chemistry, 1995. **270**(6): p. 2827-2832.
66. Ehlers, C., et al., *Functional organisation of a single nif cluster in the mesophilic arcaeon Methanosarcina mazei strain Gö1*. Archaea, 2002. **1**(2): p. 143-150.
67. Sievers, F., et al., *Fast, scalable generation of high-quality protein multiple sequence alignments using Clustal Omega*. Vol. 7. 2011.
68. Holmgren, A. and M. Bjornstedt, [21] *Thioredoxin and thioredoxin reductase*, in *Methods in Enzymology*, P. Lester, Editor. 1995, Academic Press. p. 199-208.
69. Hammel, K.E., K.L. Cornwell, and B.B. Buchanan, *Ferredoxin/flavoprotein-linked pathway for the reduction of thioredoxin*. Proceedings of the National Academy of Sciences, 1983. **80**(12): p. 3681-3685.
70. Jeon, S.-J. and K. Ishikawa, *Identification and characterization of thioredoxin and thioredoxin reductase from Aeropyrum pernix K1*. European Journal of Biochemistry, 2002. **269**(22): p. 5423-5430.
71. McCarver, A.C. and D.J. Lessner, *Molecular characterization of the thioredoxin system from Methanosarcina acetivorans*. FEBS Journal, 2014: p. n/a-n/a.
72. Grimaldi, P., et al., *Characterisation of the components of the thioredoxin system in the archaeon Sulfolobus solfataricus*. Extremophiles, 2008. **12**(4): p. 553-562.
73. Kashima, Y. and K. Ishikawa, *A hyperthermstable novel protein-disulfide oxidoreductase is reduced by thioredoxin reductase from hyperthermophilic archaeon Pyrococcus horikoshii*. Archives of Biochemistry and Biophysics, 2003. **418**(2): p. 179-185.
74. Hernandez, H.H., et al., *Thioredoxin Reductase from Thermoplasma acidophilum: A New Twist on Redox Regulation*. Biochemistry, 2008. **47**(37): p. 9728-9737.
75. Buchanan, B.B., et al., *Thioredoxin: A Multifunctional Regulatory Protein with a Bright Future in Technology and Medicine*. Archives of Biochemistry and Biophysics, 1994. **314**(2): p. 257-260.
76. Marteyn, B., et al., *The thioredoxin reductase-glutaredoxins-ferredoxin crossroad pathway for selenate tolerance in Synechocystis PCC6803*. Molecular Microbiology, 2009. **71**(2): p. 520-532.
77. Fahey, R.C., *NOVEL THIOLS OF PROKARYOTES*. Annual Review of Microbiology, 2001. **55**: p. 333-356.
78. McFarlan, S.C., C.A. Terrell, and H.P.C. Hogenkamp, *The Purification, Characterization, and Primary Structure of a Small Redox Protein from Methanobacterium thermoautotrophicum, an Archaeabacterium*. The Journal of Biological Chemistry, 1992. **267**(15): p. 10561-10569.